Influence of Multi-Stage Processing and Mechano-Chemical Treatments on the Hydration and Microstructure Properties of Recycled Aggregate Concrete

Shiv Sai Trivedi[1], Debasis Sarangi[2] and B B Das[3*], Salim Barbhuiya[4]

[1]Research Scholar, Sustainable Construction and Building Materials Laboratory, Department of Civil Engineering, National Institute of Technology Karnataka, Surathkal, Karnataka, India, 575 025, E-Mail: shivsaitrivedi@gmail.com

[2]Post Graduate Student, Sustainable Construction and Building Materials Laboratory, Department of Civil Engineering, National Institute of Technology Karnataka, Surathkal, Karnataka, India, 575 025, E-Mail: debasissarangi77@gmail.com

[3*]Professor, Department of Civil Engineering, National Institute of Technology Karnataka, Surathkal, Karnataka, India, 575 025, E-Mail: bibhutibhusan@gmail.com

[4]Senior Lecturer. Department of Engineering and Construction, University of East London, United Kingdom, University Way, London, E16 2RD, E-Mail: S.Barbhuiya@uel.ac.uk

*Corresponding Author

Abstract

On account of the shortage of naturally occurring coarse aggregate, recycled aggregate (RA) made from crushed concrete debris is now used in the construction industry. With this rise in the utilisation of recycled aggregate in the construction sector, there has been extensive research into ways to improve its quality. The significant fraction of mortar remains that are left on the RA surface is the primary factor that affects its quality. Concrete made from RA loses strength and mechanical performance due to the attached mortar's increased porosity and water absorption values and the frailer transition region between the new mortar and aggregates. In order to minimise the old cement fractions and increase the quality, this paper studies the effect of concrete incorporating multi-stage processed RA from demolished concrete waste, followed by treatment with mechanical abrasion and sodium silicate immersion. The recycled aggregates were produced through multi-stage jaw crushing, followed by utilising natural aggregate, recycled aggregate, and recycled aggregate obtained after mechanical abrasion, followed by sodium silicate treatment for concrete mix design at various substitution percentages as coarse aggregates. The experimental investigation further progresses with the evaluation of mechanical and durability properties of concrete mixes, which is additionally followed by microstructural studies such as scanning electron microscopy (SEM), Energy dispersive X-ray spectroscopy (EDAX), X-ray diffraction (XRD), Fourier transform infrared spectroscopy (FTIR), and Thermogravimetry-differential thermal analysis (TG-DTA). The outcomes demonstrate that two-stage treatment, such as mechanical abrasion followed by sodium silicate immersion, yields superior-quality RA. Recycled aggregate concrete (RAC) made with these treated aggregates illustrated an increase in workability and density with respect to an untreated RAC mix. Furthermore, comparable strengths in compression, flexure, and tension are found in treated RAC mixes, particularly at 35% replacement levels, with respect to concrete mixes comprised of natural aggregates. A similar trend is detected in the chloride penetration tests and water sorptivity tests. In addition, the microstructural investigation confirmed the formation of additional calcium silicate hydrate for treated RAC mixes, particularly for the 35% substituted RA mix. On the basis of the results, it is suggested that multi-stage jaw crushing followed by treatment through mechanical abrasion and sodium silicate can potentially enhance the mechanical, microstructural, and durability performance of RAC.

Keywords: Demolished concrete waste, multi stage processing, mechanical scrubbing, sodium silicate treatment, microstructure, recycled aggregate concrete, sustainability.

Highlights

1. Demolished concrete waste can be potentially utilised as recycled aggregates (RA).
2. Multi-stage jaw crushing followed by mechanical scrubbing and sodium silicate treatment enhances the quality of concrete RA.
3. RAC incorporating mechanical abrasion followed by sodium silicate-immersed RA shows significant improvements in density, workability, mechanical properties, and durability compared to untreated RA.
4. Additional C-S-H formation is observed at 35% replacement of two-stage treated RAC mixes through microstructural analysis.

92

LIST OF ABBREVIATIONS

RAC-Recycled aggregate concrete

RA- Recycled Aggregate

RCA- Recycled concrete aggregate

GGBS- Ground granulated blast furnace slag

SF- Silica fume

SCMs- Supplementary cementitious materials

RHA- Rice husk ash

FA- Fly ash

TSMA- Two stages mixing approach

NS- Nano silica

C&D – Construction and demolition

ITZ- Interfacial transition zone

CDW- Construction and demolition waste

SEM- Scanning electron microscopy

EDAX-Energy dispersive X-ray spectroscopy

XRD- Xray diffraction

FTIR- Fourier transform infrared spectroscopy

TGA- Thermogravimetric analysis

93

1. Introduction

Due to the demolition of outdated structures and the waste concrete from ongoing construction, crushed concrete is now widely available [1]. The primary reasons for this increasing debris may be attributed to the technical state and an end to the service life of the buildings and other such concrete structures [2]. In addition, rapid urbanisation, industrial development, and rising Populations in both developing and developed nations are creating enormous amounts of construction and demolition waste (CDW) [3]. At a global scale, the major CDW-generating nations are China and Russia, the US, and India, with an annual waste generation rate of 1020 million metric tonnes, 600 million metric tonnes, and 400 million metric tonnes, respectively [4]. Further, it is reported by several studies that the constant accumulation of CDW causes landslides, land and water pollution [5], and rising landfill costs [6–8]. On the contrary, the continuous depletion of natural aggregates and shortage of available land sites are creating grave concerns for governmental bodies. Henceforth, the adoption of recycled aggregates can simultaneously provide a sustainable solution to depleting natural resources and maintain ecological balance.

The utilisation of recycled aggregates has already been adopted by various nations [9]. However, it is found that the RA results in poor mechanical and durability performance. The primary reason for the inferior performances is the occurrence of old cementitious mortar on RA, which makes it porous and vulnerable to higher water absorption and increasing strain rates [9–16]. This can be further understood by the fact that the old mortar fractions result in a weaker old Interfacial transition zone (ITZ) compared to the new ITZ that is formed between new cement paste and aggregates. The old ITZ is found to consist of several microcracks and ettringite, whereas the new ITZ is observed to show additional C-S-H that makes it dense and contributes to better strength characteristics in RAC [14, 16–18]. Therefore, it becomes imperative to adopt suitable processing and treatment methods for the sustainable incorporation of RA [4]. The processing techniques adopted by various authors include crushing, screening, and contamination removal, if any [10, 19, 20]. In particular, the crushing of RA can be done through a jaw crusher, impact crusher, cone crusher, roll crusher, etc. [21–25]. Among these crushers, the widely used crushing systems comprise jaw and impact crushing. It is to be noted that the selection of crushers becomes an important parameter in producing RA as it has a direct influence on aggregate shape, size, and respective distribution characteristics [26]. Further, a two-stage crushing process, i.e., jaw crushing followed by hammer milling, yields superior RA, particularly for better mechanical performances in RAC [27].

Florea [1] investigated the effect of multi cycle jaw crushing (10 crushing cycles) on RA and it was found that additional amount of cement paste was recovered by increasing number of crushing cycles. However, the additional number of crushing cycles were more energy consuming than the ordinary crushing process. Hence, it is necessary to explore the optimum number of crushing cycles for processing RA.
Treatment options for RA include removing attached mortar or its surface coating, improving the binder, consolidating adherent mortar, and improving the microstructure between fresh mortar and RA. etc [2]. A detailed review of the various treatment methods adopted for RA is shown in Table 1. It can be observed that the studies based on abrasion or sodium silicate-based treatment resulted in durable RAC and provides notable curtailments in water requirements of RA that in one of a major concern in demolition-based materials. However, a combined study is required to evaluate the effect on mechanical and microstructure performance of the mechano-chemical treated RA for the development of RAC. In addition, carbon dioxide curing and nano particle also helps to strengthen the remnant mortar by significantly reducing the water absorption and porosity of the RA [3–5]. Numerous methods, including mechanical grinding of RA [6,7], heat grinding of RA [8], and pre-soaking solutions [9,10] , may be employed to remove remnant RA mortar. However, there found to be certain disadvantages by incorporating above techniques such as insignificant durability properties [8], growth in chloride and sulphate ions [11], enormous energy expenditures and increasing levels of carbon dioxide discharges [3], etc. In view of the limitations associated with above techniques, the application of mechanical abrasion would provide an effective and efficient removal approach for the remnant mortar fractions. In addition, it is observed that sodium silicate immersion helps to limit the permeation of chloride ions, reduces water absorption and produces a denser ITZ at microstructure level [12]. Henceforth, there is a need to explore the collective effect of mechanical scrubbing and sodium silicate (mechanical-chemical treatment) treated RA for the sustainable production of RAC.

Recycled concrete aggregates may be utilized at maximum 25% and 20% for M 25 grade plain and reinforced mixes respectively according to IS: 383 [39], as per amendment in early 2016. The requirements for using coarse and fine RA while producing various types of concrete are shown in Table 2. RCA may be used in concrete for bulk fills, bank protection, base/fill of drainage structures, pavements, sidewalks, kerbs and gutters, etc., according to the National Building Code (NBC-CED 46) of India 2005, Part 11 of NBC 2005 on 'Approach to Sustainability' (Chapter 11) [40]. When RA is substituted for control aggregate, it has been observed to increase compressive strength by 0% to 40% [41].

However, there is no observed fall in strength for concrete having up to 20% fine or 30% coarse RCA. However, once RA concentration increases above these fractions, there is a orderly reduction in strength is observed in a study [42]. When compared to control concrete, the qualities of RAC produced of 100% RA have been found to be significantly reduced, however the characteristics of RAC incorporated of a mixture of 75% NA and 25% RCA exhibited no discernible modification in concrete performances. [13]. Henceforth, this research work attempts to explore the substitution effect of treated coarse RA post 30% replacement for the sustainable development of RAC.

In this current research work, the potential of mechanical-chemically treated RA as a coarse aggregate in the development of RAC is investigated. The C&D waste is first processed to obtain the requisite RA, which is then treated using mechanical and chemical processes to develop treated RAC that has various ratios of treated coarse RA. For this experimental research, four distinct concrete mix designs have been used. In comparison to control concrete and untreated RAC mix, the research explores the optimal mix design for treated RAC in terms of fresh and hardened-state concrete properties and durability characteristics. The impact of the optimal treatment method on the microstructure of RAC is further examined, and it is contrasted with both control concrete and untreated RAC mix. The paper also analyses the drawbacks of mechanical-chemical treatment and proposes suggestions for enhancing the sustainability measures of the adopted treatment.

180

Table 1. Comparative review on various treatment methods on RA

Treatment method	Parameters and Influences					References
	Chloride ingress in RAC	Water absorption In RAC	Resistance to Corrosion or electrical conductance	Relative strength in compression [b]	Relative cost [a]	
Incorporating SCMs (GGBS+SF)	Reduces chloride ingress between (13-53%)	Reduces water absorption up to 8%	Insignificant consequence	--	--	[14,15]
Incorporating ground rice husk ash (GRHA)	Provide resistance to Chloride ingress	--	Enhances resistance against steel corrosion	--	--	[14,16]
Incorporating RHA	Provide resistance to Chloride ingress	Reduces water absorption	--	--	--	[14,17]
Admixing SF	Reduces chloride ingress till 60%	Reduces water absorption up to 41%	Enhances electrical resistivity by 3.4 times	--	--	[14,18]
Incorporating GGBS	Reduces chloride ingress between (28-67%)	Reduces water absorption	Equivalent corrosion resistance to control concrete	--	--	[14,19]
Incorporating FA	Reduces chloride ingress	Reduces water infiltration	Corrosion density comparable to NAC at later age	--	--	[14,20]
Incorporating SCMs+ TSMA	Reduces chloride ingress by 59%	--	Enhances resistance against steel corrosion	1.24	1.00	[14,15,21–27]
Los angeles abrasion	Reduces chloride	Reduces water	--	1.15	1.00	[14,21–28]

	ingress by 24%	absorption up to 4%				
Collective treatment using sodium silicate+ SF	Reduces chloride ingress by 80%	--	--	--	--	[12,14]
Collective treatment using carbonation+ Nano silica (NS) spray	Reduces chloride ingress by 24%	Substantial reduction in water absorption rates	--	--	--	[14,26]
NS spray methods	Reduces chloride ingress by 3.8%	--	--	1.12	1.44	[14,15,21–27]
Surface treatment with slurry (cement+ NS)	Reduces chloride ingress by 15%	Reduces absorption to 6%	--	--	--	[14,29]
Nano materials induced surface treatment	Reduces chloride ingress by 10%	--	--	--	--	[14,29]
Carbonation treatment	Reduces chloride ingress by 26%	Reduces absorption by 29%	Enhances resistance against steel corrosion	1.09	2.05	[14,15,21–26,28,30]
SF slurry	Reduces chloride ingress by 41%	Reduces absorption to 22%	Enhances electrical resistivity by 60% (approximately)	1.55 (with FA)	1.04 (with FA)	[14,15,21–26,28,31]
Pre-soaking in NS solution	Reduces chloride ingress by 61%	Reduces sorptivity by 58%	--	1.42	1.15	[14,15,21–25,28]

[a] Relative cost (per m^3) is defined as the ratio of cost of treated RAC to the cost of untreated RAC on 100% substitution of RA in RAC

[b] Relative strength in compression is defined as ratio of strength in compression of treated RAC to strength in compression of untreated RAC

Table 2 IS 383: 2016 Coarse and Fine Aggregate for Concrete Specification

C&D Waste	Plain Concrete	Reinforced Concrete (Up to M25)	Lean Concrete (<M15)	Extent Of Utilization
Recycled Concrete Aggregate	25%	20%	100%	As Coarse Aggregates
Recycled Aggregate (RA)	NIL	NIL	100%	As Coarse Aggregates
Recycled Concrete Aggregate (RCA)	25%	20%	100%	As Fine Aggregates

2. Experimental Program

2.1 Materials Used

2.1.1. Preparation of RCA

The source of recycled concrete aggregates (RCA) is the demolished waste concrete cubes from the structural and materials laboratory at NITK, Surathkal, India (13.0108° N, 74.7943° E). The demolished concrete wastes were first cleaned, followed by size reduction through manual hammering. A detailed processing methodology is summarised in Fig. 1. It is to be noted that multiple crushing cycles were adopted for minimising adhered mortar content and simultaneous procurement of coarse RA. The crushed sample was further sieved through an appropriate size fraction for acquiring coarse RA fractions referring to the sustainability measures of the adopted treatment.

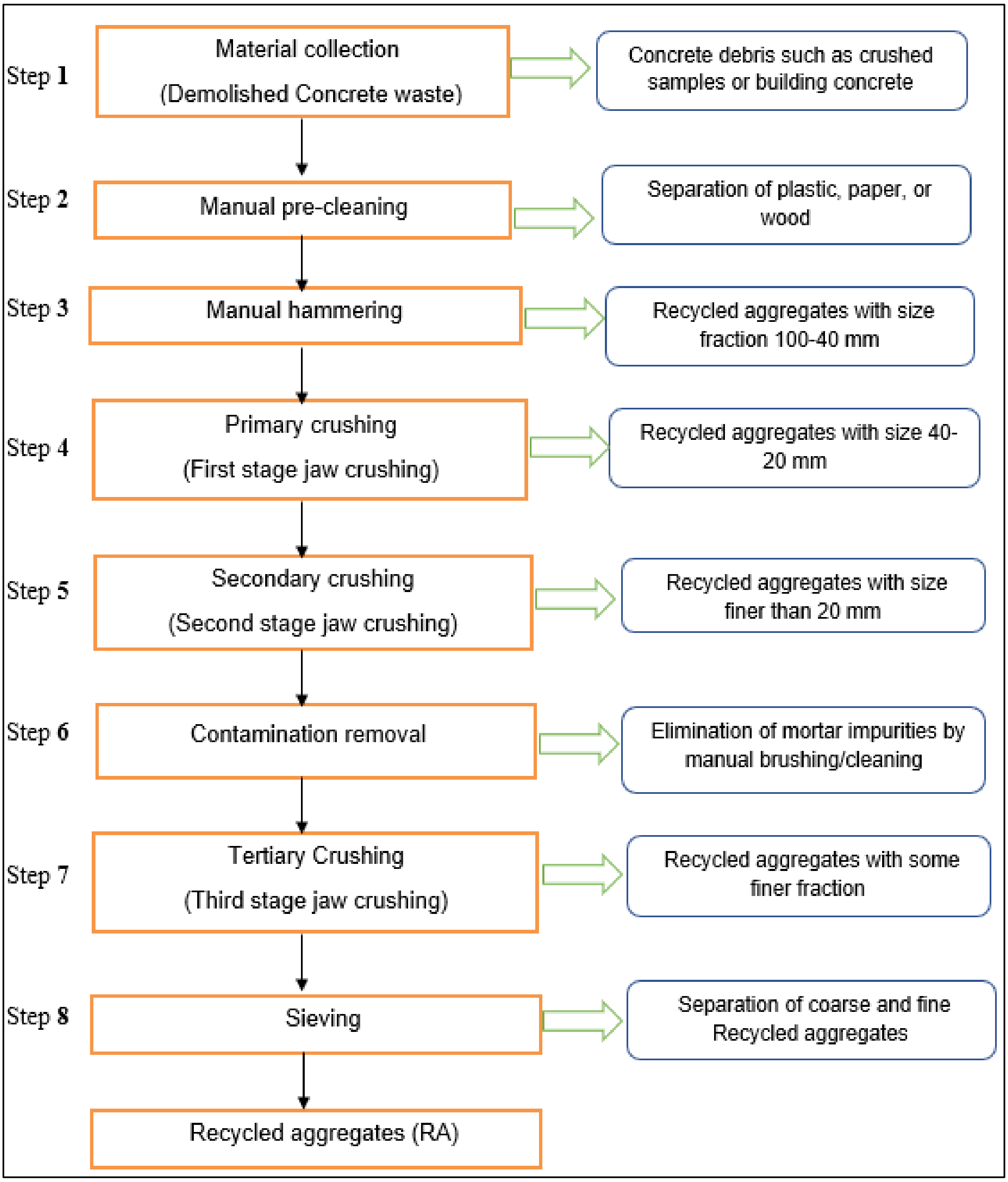

Fig. 1. Multi stage processing technology for recycled concrete aggregates

2.2 Mechanical-Chemical treatment of Recycled Aggregate

Four distinct RAC mixes were explored in this research work. A couple of RAC mixes were designed by incorporating mechanical-chemical treated coarse RA at different substitution percentages of 35% and 50%. The mechanical-chemical treated RAC mixes are designated by the substitution percentage of treated coarse RA, i.e., TR3 and TR5 for 35% and 50% replacement respectively. Additionally, two other types of RAC mixes were used as control mixes for assessing the usefulness of mechanical-chemical treatment, i.e., NAC and RAC in absence of any treatment methods (100% untreated coarse RA-URAC).

2.2.1 Mechanical Scrubbing

For the mechanical-chemical treatment of RA, a two-step procedure was used, as indicated in Fig. 2. The Los Angeles testing device is filled with 10 kg of processed RA and rotated for 17 minutes at a speed of 33 revolutions per minute (rpm) without any additional charges [32]. In the absence of mild steel balls, spinning was permitted to continue. The collision partially dislodged the fragmented mortar that was adhering to the aggregate surface. The aggregates were sieved when the rotating period was over, and the 12.5 mm retained aggregates were gathered. The chosen mechanical treatment makes sure that any old cementitious mortar is removed and gives the treated RA of uniform qualities.

2.2.2 Chemical treatment

In this step, the aggregates obtained after mechanical scrubbing was further treated with sodium silicate (Na_2SiO_3) solution. The aggregates were cleaned with water and immersed in 20%Na_2SiO_3 solution then mixed for 1 hour [27] . Then the aggregates were detached from the solution and air dried for 24hrs. Waterglass treatment and pore blocking surface treatment are other names for this procedure. The sodium silicate treatment works on the induced chemical reaction between sodium silicate and old cementitious mortar on RA to produce C-S-H that is found to be effective in strengthening the mortar remains and blocking the capillary pores in concrete surfaces, as shown in equation 1.

$$\boxed{Na_2O.\,SiO_2 + Ca(OH)_2 \rightarrow CaO.\,nSiO2.\,xH_2O\ (Gels) + 2NaO} \tag{1}$$

Sodium silicate	Hydration product from adhered mortar fractions	C-S-H gel (strengthening the adhered mortar remains)

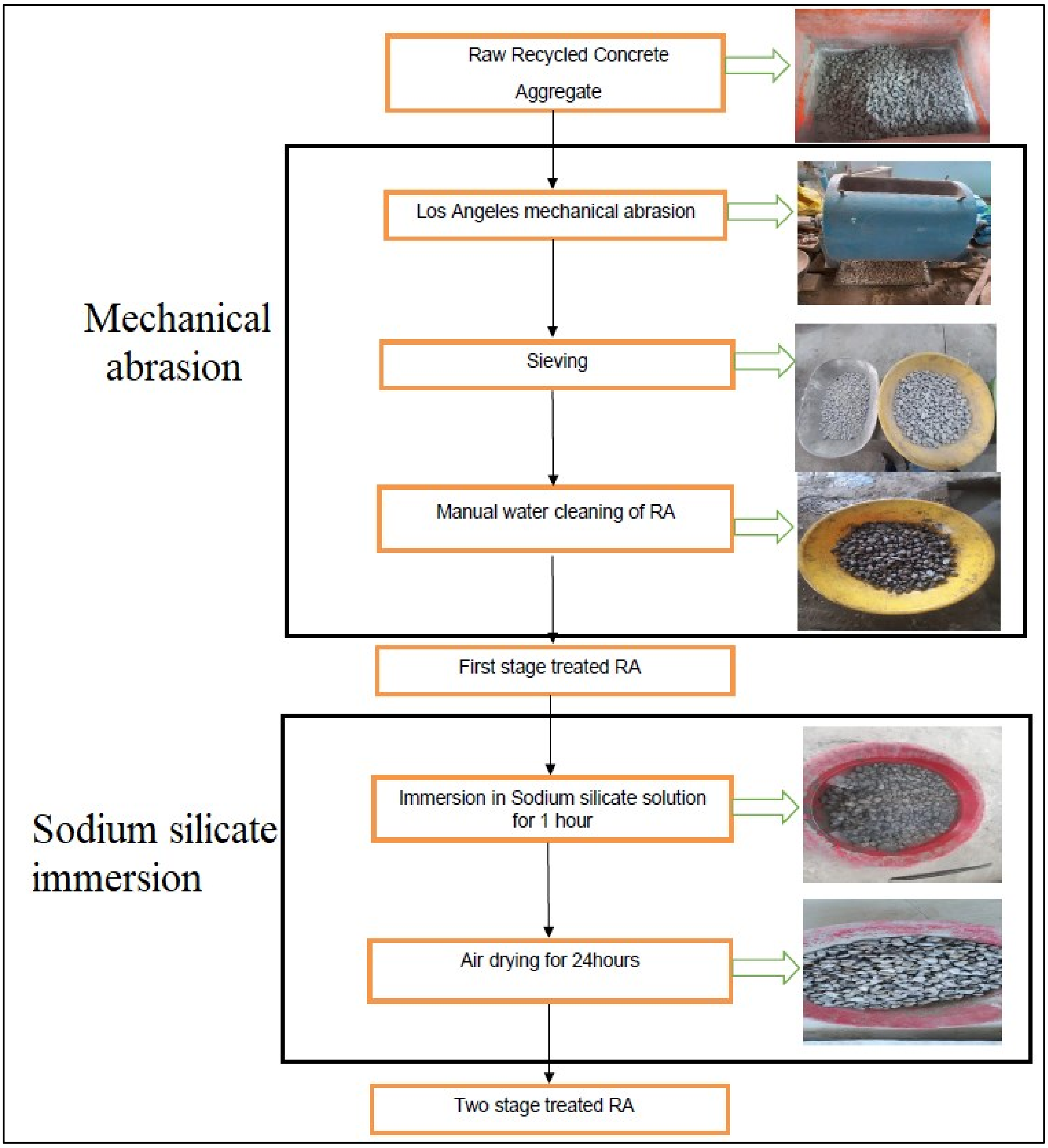

Fig. 2. Multi stage treatment process for recycled concrete aggregates

2.3 Physical performance of aggregates

The specific gravity, water absorption, bulk density as per IS 2386- Part 3, aggregate crushing value, aggregate impact value as per IS 2386 - Part 4, and aggregate abrasion value of all treated RA(s) were evaluated. Additionally, the physical characteristics of RA were compared to the IS 383 requirements for coarse aggregate. Comparative analysis is done to evaluate the efficacy of mechanical and chemical treatment in two stages on recycled concrete aggregates. Table 3 provides an illustration of these aggregates' physical characteristics.

2.4 Mix Design for control, treated and untreated RAC mixes

M40 grade mix design for all four concrete specimens was adopted as per the specifications mentioned in IS 10262:2009 and the detailed mix design is presented in Table 4. Overall, 4 distinct mixes were produced for different percentage replacement of RCA as coarse aggregate in mixes. The mix designation was made as NAC, URAC, TR3 and TR5 for mix 1, mix 2, mix 3 and mix 4 respectively. Here NAC represents natural aggregate concrete, URAC represents 100% replacement of untreated recycled concrete aggregates, TR3 represents 35% replacement of treated recycled concrete aggregates, TR5 represents 50% replacement of treated recycled concrete aggregates. It is noteworthy that the design mix is depicted for coarse aggregates under saturated surface dry (SSD) conditions and the concrete cubes were vibration cast followed by water curing in the tanks.

Table 3. Physical properties of aggregates

Properties	Natural Aggregates	Untreated RA	MS+SS_RA	SS_RA
Bulk Density(loose) Bulk Density(compacted)	1490 Kg/m^3 1498 Kg/m^3	1284 kg/m^3 1293.3 kg/m^3	1346 kg/m^3 1355 kg/m^3	1307 kg/m^3 1314 kg/m^3
Specific Gravity	2.69	2.56	2.63	2.52
Water absorption	0.6%	3.6%	1.05%	2 %
Aggregate Impact value	18%	28%	19.82%	24.29 %
Aggregate Crushing Value	15%	39.2%	22.64%	29.04 %
Los angeles abrasion value	20%	25.6%	22.02%	25.14 %

Table 4 Mix proportion of concrete for 1 m^3

Mix	w/c	Natural Aggregate (%)	Cement (kg/m^3)	Water (kg/m^3)	Coarse Aggregate (kg/m^3)		Fine Aggregate (kg/m^3)
					Natural	Recycled	681.95
Mix 1	0.4	100	493	197	1028.74	0	681.95
Mix 2	0.4	0	493	197	0	1028.74	681.95
Mix 3	0.4	35	493	197	360.06	668.68	681.95
Mix 4	0.4	50	493	197	514.37	514.37	681.95

2.5 Testing of concrete mixes

The impact of the four distinct mix types on the concrete's compressive strengths after seven and twenty-eight days was examined as per IS 516 [33] . Additionally, impacts of these mixes on slump value, split tensile strength, flexural strength, and density of concrete were examined as per IS 1199, IS 5816 and IS 516 respectively [33–35] . For the durability performance of mixes, a couple of tests were performed such as rapid chloride penetration test (RCPT) and water sorptivity tests as per ASTM-C1202 and ASTM-C1585 respectively [36,37].

2.6 Microstructure studies

The microstructure studies of different concrete mixes were accomplished through SEM, EDAX, FTIR, XRD and TG-DTA. Chunks from concrete samples were collected followed by crushing and sieving and then oven dried for the analysis of aforementioned studies. Images were obtained through scanning electron microscope (GEMINI 300, Carl Zeiss, Resolution: 0.7 nm @15 kV, 1.2 nm @1 kV) and elemental analysis was conducted through an EDAX analyzer to know the change in elemental composition within the boundary of image. The XRD analysis is done using Malvern PANalytical at Central research facility (CRF), NITK at deflection angle ranging from 4 to 80 and at a scanning speed of 2/min. The X'Pert High Score Plus software was then used to analyze the discovered patterns. FTIR analysis was carried out utilizing a Bruker (Alpha II) instrument with a resolution of 2 cm^{-1} and a wavenumber range of 4,000 to 500 cm^{-1}. A Rigaku TG-DTA 8122 TG/DTA analyzer was used to perform TGA. Within the range of 25°C to 900°C, samples were placed inside the analyzer at a heating rate of 10°C/min in a nitrogen purge environment (purge rate: 10 mL/min).

3. **Results and discussions**

3.1 Physical properties of treated RA

3.3.1 Specific gravity and bulk density

Fig. 4 illustrates the specific gravity of multi-stage treated RA, untreated RA, and natural aggregate. It is evident that treated RA has a higher specific gravity than untreated RA, but less specific gravity than NA. Further, a similar observation (Fig. 3) may be noted for the bulk density measurements of mechanical -chemical treated aggregate that has higher bulk density as compared to untreated RA but fewer value than natural aggregate.

The removal of adhering mortar from mechanical scrubbing treatment, which is weak and porous in nature, may have caused the increase in specific gravity. In addition, sodium silicate solution strengthens the recycle aggregates by converting adhered mortar to C-S-H. The increase in bulk density further confirms the above observation as specific gravity represents the denseness of aggregates. The probable reason in the increase in bulk density of multi stage treated RA may be attributed to the stronger coating of sodium silicate that increases the denseness of aggregate. Also, the SEM investigations in this study confirms the establishment of a dense microstructure owing to the development of C-S-H fractions. This conclusion agrees with observations from Guneyisi et al. [38] that studied the effect of sodium silicate as surface treatment methods for the development of self-compacting concrete incorporating RA. IS 383 [39] recommends the incorporation of dense aggregates in constructional works henceforth the observations from specific gravity and bulk density indicates that mechanical-chemical treated RA are of superior quality than untreated RA.

3.3.2 Water absorption

Figure 4 depicts the water absorption of multistage treated RA, untreated RA, and natural aggregate. It can be seen that treated and untreated RA exhibit significantly different water absorption values, with treated RA absorbing only around 30% water content than untreated RA, however in comparison to the natural aggregates, treated RA still illustrates higher water absorption. This outcome may be attributed to the dense coating formed as a result sodium silicate immersion on the surface of RA. With a dense coating, the pores are getting clogged and filled up with the sodium silicate solution. The water-based silicate gel (C-S-H gel) is formed as a reaction between calcium hydroxide and sodium silicate solution resulting a dense matrix.

This conclusion agrees with observations from [38,40] where the RA treated with sodium silicate solution reported a fall in the water absorption values particularly with respect to the untreated RA. IS 383 [39], recommends that pre wetting is not required with RA having water absorption values fewer than 5 percent. Henceforth, multi stage treated RA may be used in concrete applications without requirements of pre wetting.

3.3.3 Aggregate crushing value, impact value and abrasion value

The Aggregate crushing value, impact value and abrasion value of the multi stage treated RA along with untreated RA and natural aggregate is shown in Fig. 5. It is evident that treated RA has a lower crushing, impact, and abrasion value than untreated RA, but slightly greater values than NA. This observation may be attributed to the weakening and removal of adhered mortar post mechanical scrubbing. Moreover, the application of sodium silicate is filling the pores and microcracks inside aggregate and resulting an improvement in the aggregates performance in crushing, impact, and abrasion value. This investigation is in line with the investigation led by He et al. [40] in which the aggregate crushing value is getting decreased from the incorporation of sodium silicate treatment.

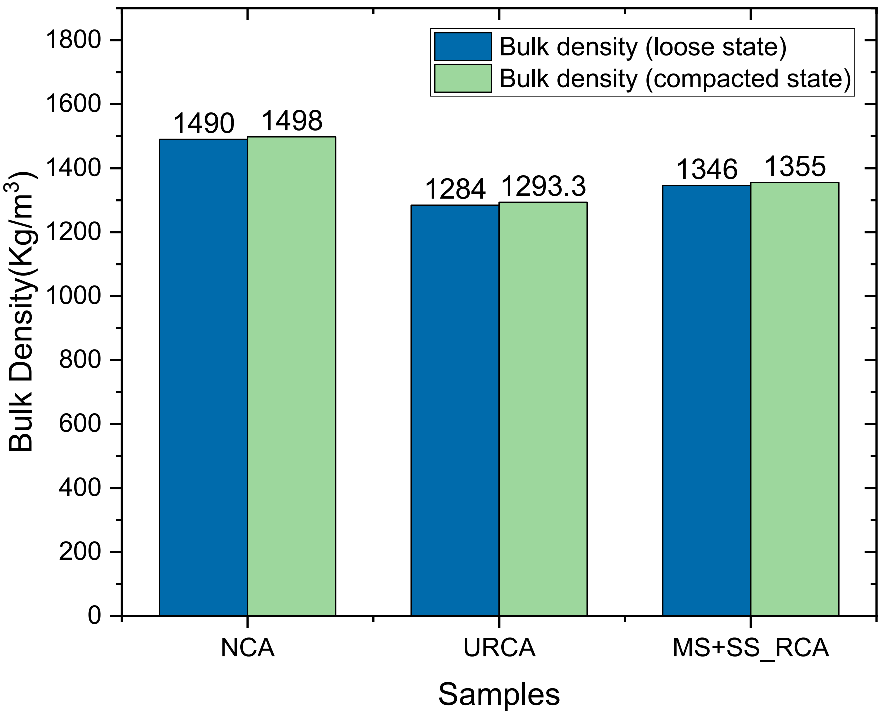

Fig. 3. Bulk density of treated and untreated RA

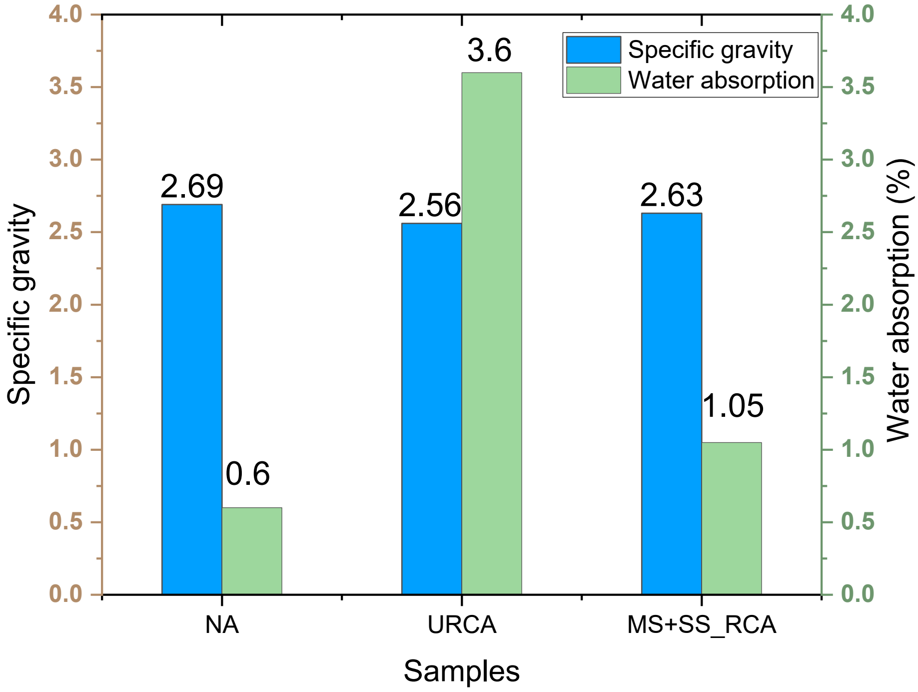

Fig. 4. Specific gravity and water absorption of treated and untreated RA

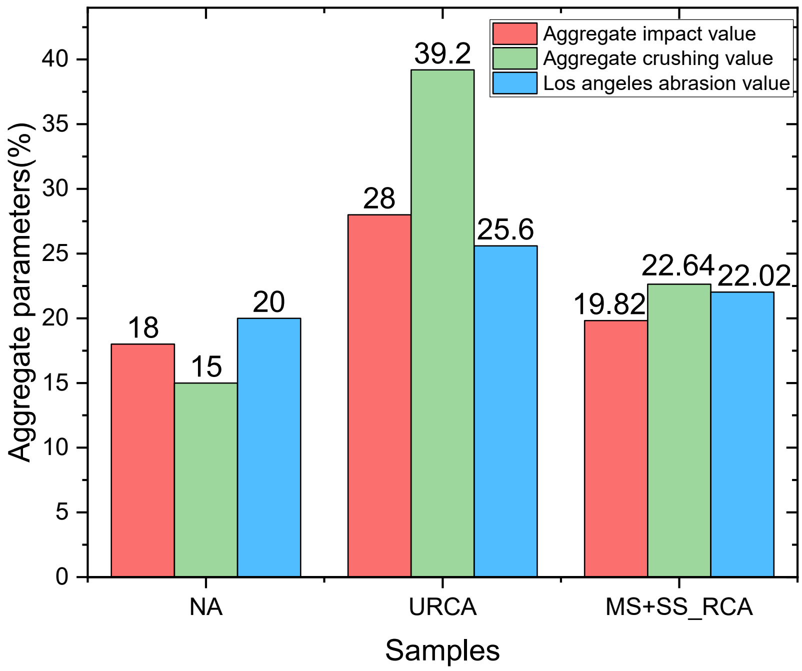

Fig. 5. Aggregate impact, crushing and abrasion values of treated and untreated RA

3.2 Effect of multi stage treated RA on development of RAC

3.2.1 Density

Fig. 6 shows the density of RAC mixes incorporating mechanical-chemical treated RA (TR3, TR5), untreated RA (URAC) and control aggregates (NAC). Specifically, the densities of NAC, TR3, TR5 and URAC were observed as 2450 kg/m^3, 2432 kg/m^3, 2420 kg/m^3 and 2385 kg/m^3 respectively. It can be detected that URAC specimen illustrates lowest density and NAC acquires highest density whereas the treated RAC mixes depict comparable density to that of NAC mix. However, the density of RAC (TR5) decreased after adding additional treated RA. This observation may be attributed to the bulk density of RCA that is fewer to that of control aggregates due to the presence of porous adhered mortar. The attached mortar reduced after the two-stage treatment that assists to an increment in the bulk density of RA which in turn increases the density of concrete mix. Therefore, the optimum density is obtained at 35% replacement of mechanical-chemical treated RA in concrete mixes.

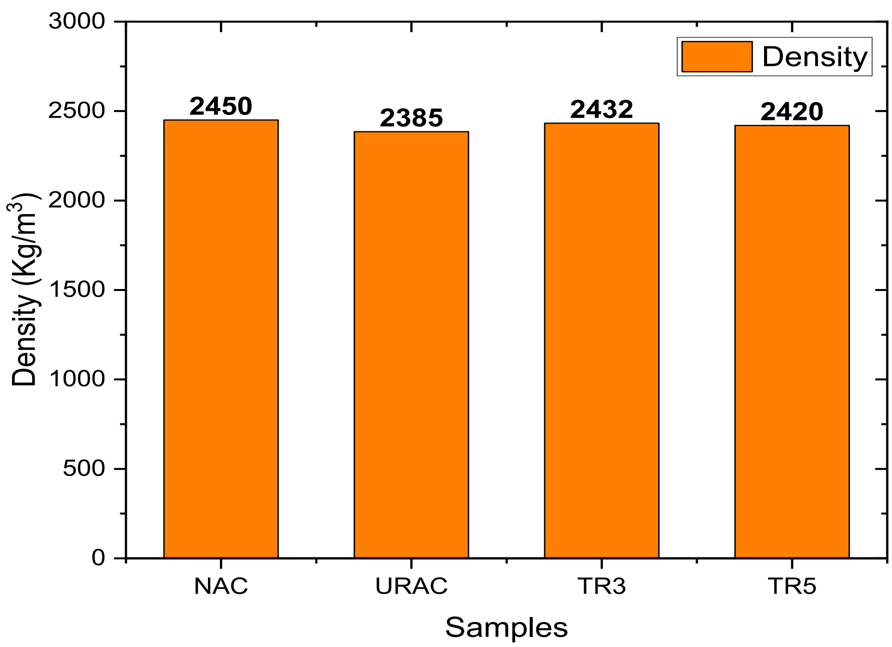

Fig. 6. Effect of treated RA on density of concrete mixes

3.2.2 Workability

Fig. 7 shows the slump values (workability) of NAC, URAC, TR3 and TR5 mixes. Specifically, the slump values of NAC, URAC, TR3 and TR5 were observed as 80 mm, 26 mm, 50 mm, and 36 mm, respectively. It can be detected that URAC specimen illustrates lowest workability and NAC mix acquires highest workability, whereas the treated RAC mixes depict an improvement in the slump values to that of URAC mix, particularly at 35% substitution levels that results nearly twice the slump. However, the slump values of RAC (TR5) decreased after adding additional treated RA but reports better values to that of URAC mix. This observation may be attributed to the addition of RA that made the mix harsher and less flowable. Utilizing raw RA weakens the lubricating effect of cement paste, making the movement of aggregates more difficult. As the percentage of RA increased, it absorbed some water due to adhered mortar and the workability of the mixes get reduced. On the contrary, the two-stage treated RA eliminated the porous adhered mortar fractions and a dense coating of sodium silicate blocked the pores of aggregate and provided an increment in slump values of treated RAC mixes.

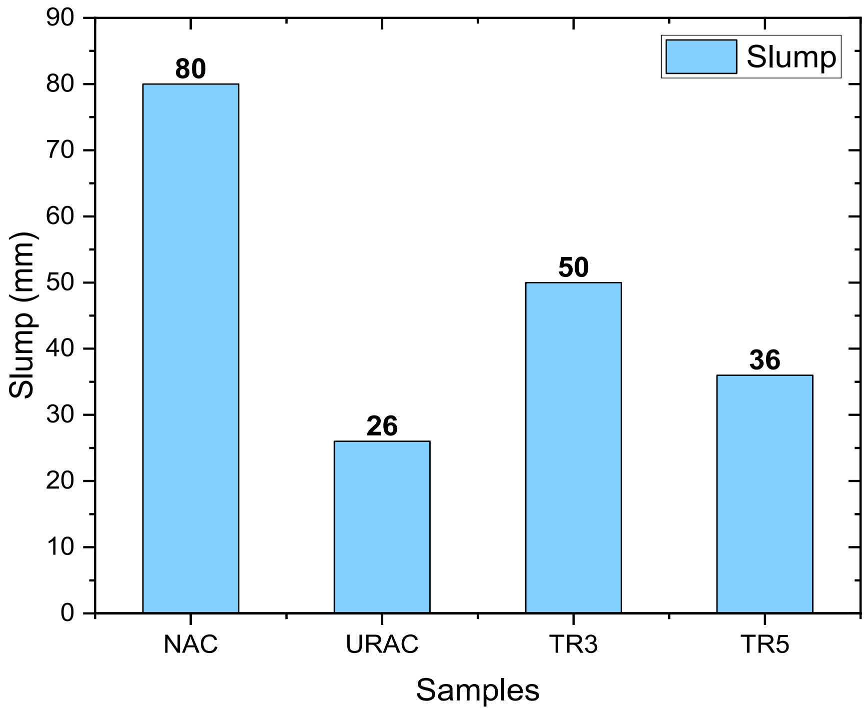

Fig. 7. Effect of treated RA on workability of concrete mixes

3.2.3 Compressive strength

Fig. 8 shows the compressive strength of NAC, URAC, TR3 and TR5 mixes. Specifically, the 7 days compressive strength values of NAC, URAC, TR3 and TR5 mixes were observed as 39.4 MPa, 29.55 MPa, 35.14 MPa, and 34 MPa, respectively whereas the 28 days compressive strength values of NAC, URAC, TR3 and TR5 mixes were observed as 55.55 MPa, 42.22 MPa, 50.21 MPa, and 48.58 MPa, respectively. It can be detected that URAC specimen illustrates lowest compressive strength at 7 days and 28 days and NAC mix acquires highest strength in compression at same aging, whereas the treated RAC mixes depict comparable strength to that of NAC mix, particularly at 35% substitution levels. However, the compressive strength of RAC mix (TR5) slightly decreased after adding additional treated RA but reports better values to that of URAC mix. The increase in compressive strength due to treatment methods is in line with observations from Pandurangan et al. [41] with the obtained strength in treated RAC specimen is in range of 88-92 % to that of NAC mixes. Also, the slight fall in compressive strength from TR3 mixes to TR5 mixes is an indication of 35% as an optimum substitution of treated RA in the development of sustainable RAC mixes. Further, owing to the permeable features of the old cementitious mortar remains on untreated RCA, and weak old ITZ, develops additional vulnerable sites in concrete, that ultimately produces an inferior compressive strength in URAC mixes as compared to NAC. Nevertheless, with multi stage treatment, this adhered mortar is getting minimized followed by a dense coating of sodium silicate solution that results a strong ITZ at microstructure levels.

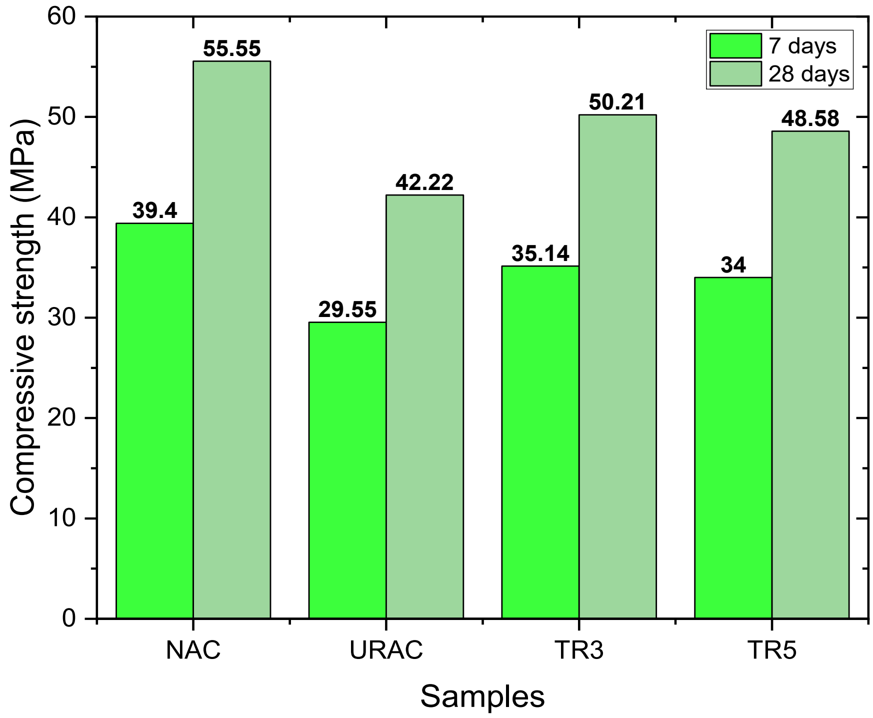

Fig. 8. Effect of treated RA on compressive strength of concrete mixes

3.2.4 Split tensile strength and flexural strength

Fig. 9 shows the flexural and split tensile strength of NAC, URAC, TR3 and TR5 mixes. Specifically, the 28 days flexural strength values of NAC, URAC, TR3 and TR5 mixes were observed as 8.75 MPa, 4.5 MPa, 6.75 MPa, and 5.58 MPa, respectively whereas the split tensile strength value at same aging of NAC, URAC, TR3 and TR5 mixes were observed as 4.28 MPa, 3.1 MPa, 3.86 MPa, and 3.57 MPa, respectively. It can be detected that URAC specimen illustrates lowest flexural and split tensile strength at 28 days and NAC mix acquires highest strength in flexure and split tensile strength at same aging, whereas the treated RAC mixes depict comparable strength to that of NAC mix, particularly at 35% substitution levels. However, the flexural strength and split tensile strength of RAC mix (TR5) slightly decreased after adding additional treated RA but reports higher values to that of URAC mix. This observation was accredited to weak bonding amid old and new cementitious matrix. Nevertheless, with two stage treatment, the adhered mortar remains gets removed from aggregate surface by continuous mechanical abrasion cycles followed by development of a strong ITZ as a result of sodium silicate immersion.

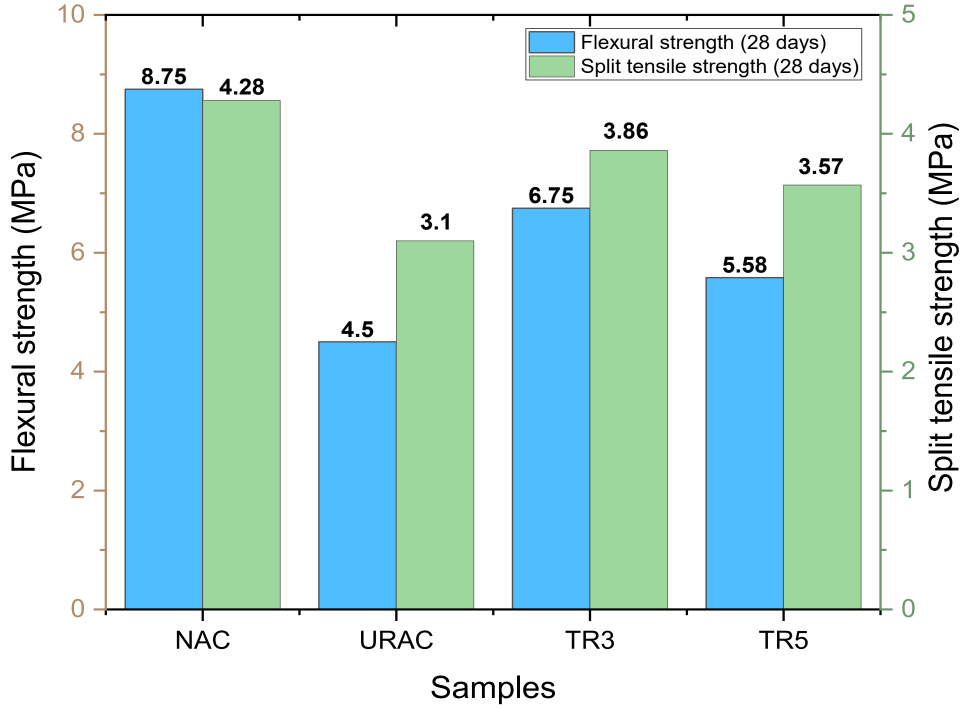

Fig. 9. Effect of treated RA on flexural and split tensile strength of concrete mixes

3.2.5 Durability of treated and untreated RAC mixes

3.2.5.1 Chloride penetration

Fig. 10 shows the chloride penetration values of NAC, URAC, TR3 and TR5 mixes. Specifically, the chloride penetration (in coulombs) of NAC, URAC, TR3 and TR5 were observed as 2950 C, 4300 C, 2780 C, and 2650 C, respectively. It can be detected that URAC specimen illustrates highest chloride penetration and treated mixes i.e., TR3 and TR5 mixes acquires lowest chloride penetration, whereas the NAC mixes depict a sharp fall in the chloride penetration to that of URAC mix. This finding may be explained by the fact that a higher percentage of untreated RA increased the specimens' porosity, particularly in terms of increasing the occurrence of microcracks on the transition zone between the RCA and the cement paste, which is significant for the transport mechanisms of concrete and results in greater chloride migration. Incorporation of multi stage treated RCA exhibits more resistivity to chloride ion permeability than NAC specimen owing to the occurrence of additional calcium silicate hydrate, which assists in chloride binding.

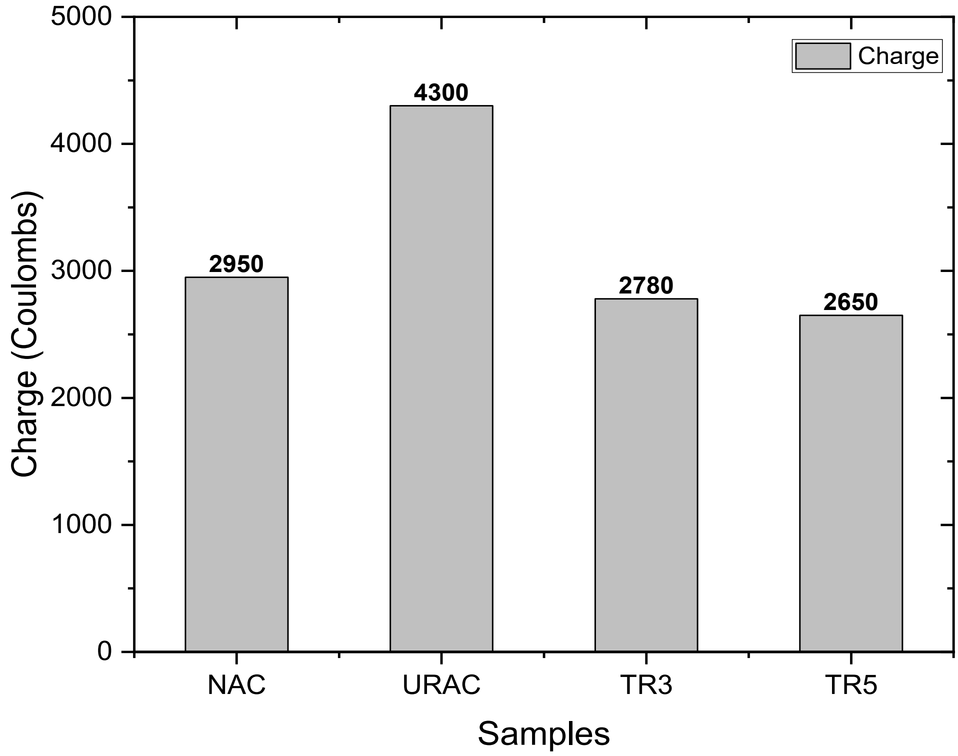

Fig. 10. Effect of treated RA on rapid chloride penetration values of concrete mixes

3.2.5.2 Sorptivity

Fig. 11 shows the water sorptivity values of NAC, URAC, TR3 and TR5 mixes. It can be detected that URAC specimen illustrates highest absorption values particularly at secondary stages, whereas the NAC mixes depict lower absorption values that of URAC mix both at initial and secondary stages. It is worth noting that the treated RAC mixes (TR3, TR5) showing substantial decrease in water absorption values at both the stages, particularly the secondary absorption is found to be least in both the mixes with respect to the other concrete specimens. This observation may be accredited to the fact that untreated RA are porous in nature owing to the adhered mortar fractions that provides additional water absorption sites. On contrary, the multi stage treated RA shows lower water absorption values owing to the presence of negligible mortar fractions. Moreover, the dense coating of sodium silicate resists the water absorption that further results to a lower sorptivity. Table 5 shows the absorption values of different concrete specimens at various time intervals. It is to be noted that the initial absorption is considered for the points measured up to 6 hours whereas the secondary absorption is measured for the points ahead of the first day [37].

Table 5 Sorptivity data for various concrete specimens

Test Time	Time ($sec^{1/2}$)	Absorption (mm)			
Days		NAC	URAC	TR3	TR5
	0	0	0	0	0
	8	0.35233	0.38698	0.32923	0.4948
	17	0.58337	0.57181	0.54871	0.71621
	24	0.68156	0.67385	0.65075	0.80285
	35	0.76242	0.73739	0.73546	0.89719
	42	0.82403	0.79707	0.799	0.97613
	60	0.94725	0.9357	0.94917	1.14555
	85	1.13208	1.13785	1.14363	1.40547
	104	1.24759	1.26107	1.2707	1.58067
	120	1.33423	1.36311	1.38044	1.72699
	134	1.40354	1.43435	1.4536	1.83096
	147	1.42087	1.45168	1.47093	1.85599
1	304	2.00809	2.04852	2.24297	2.7628
2	440	2.28918	2.31613	2.62033	3.19022
3	518	2.4278	2.44705	2.79938	3.40585
4	657	2.63188	2.61841	2.91298	3.64844
5	726	2.73392	2.70312	3.12476	3.76781
6	789	2.78976	2.74548	3.17482	3.81402
7	831	2.84752	2.78783	3.22487	3.86022

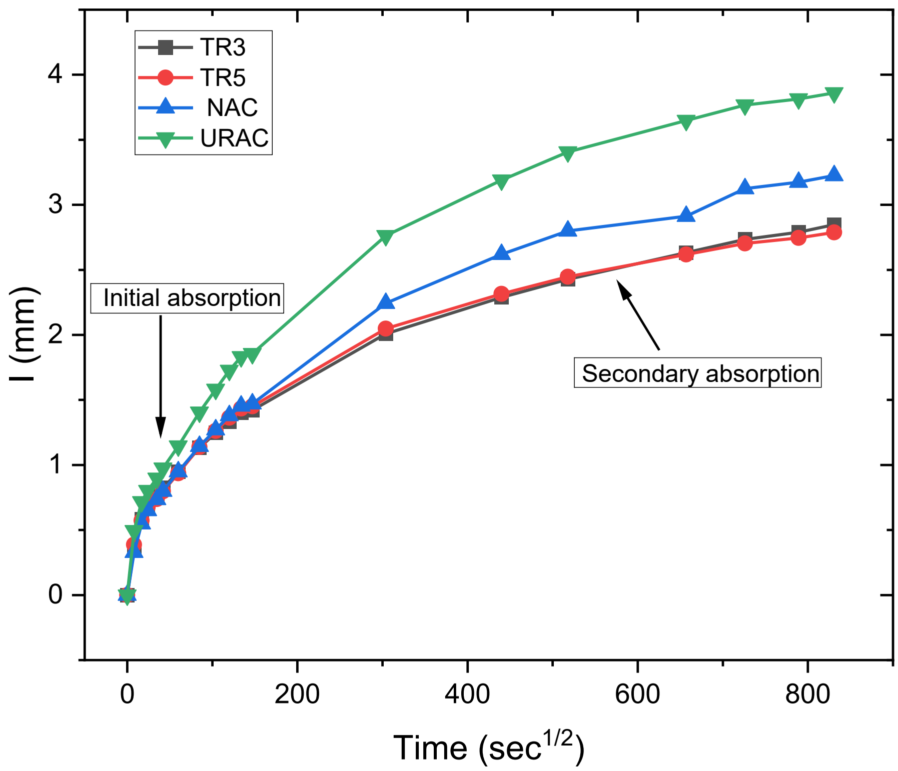

Fig. 11. Effect of treated RA on water sorptivity values of concrete mixes

3.2.6 Microstructural studies

3.2.6.1 Scanning electron microscopy (SEM)

The SEM images of NAC, URAC, TR3 and TR5 are shown in the Figs. 12-15 respectively. It can be observed that in case of NAC, there is an even distribution of all hydration phases such as ettringites, calcium hydroxides and C-S-H. A couple of voids are also illustrated through images. On the contrary, URAC specimen shows some fractions of old mortar alongside ettringites that are present in majority amount, with minimum occurrence of C-S-H. It can be accredited to the occurrence of old mortar fractions on RA surface that develops a porous and vulnerable microstructure. In case of treated RAC mixes such as TR3 and TR5, the presence of C-S-H is predominant alongside a few cracks that are owing due to the mechanical abrasion cycles. An auxiliary C-S-H formation is a consequence of reaction between adhered mortar and sodium silicate that provides a dense and even surface coating. However, with increased percentage of treated RA fractions, an unevenness is observed.

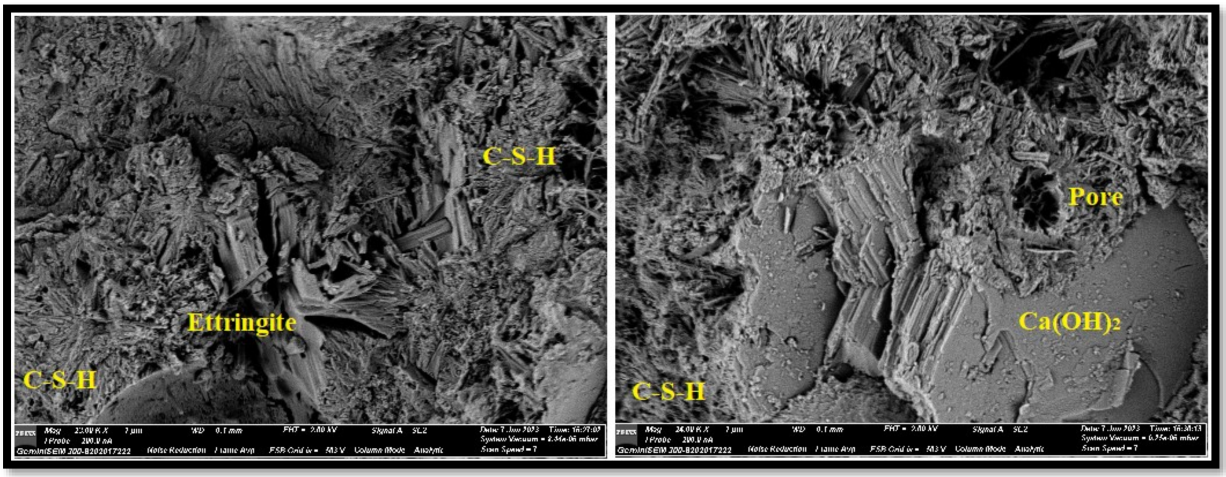

Fig. 12. SEM images of NAC

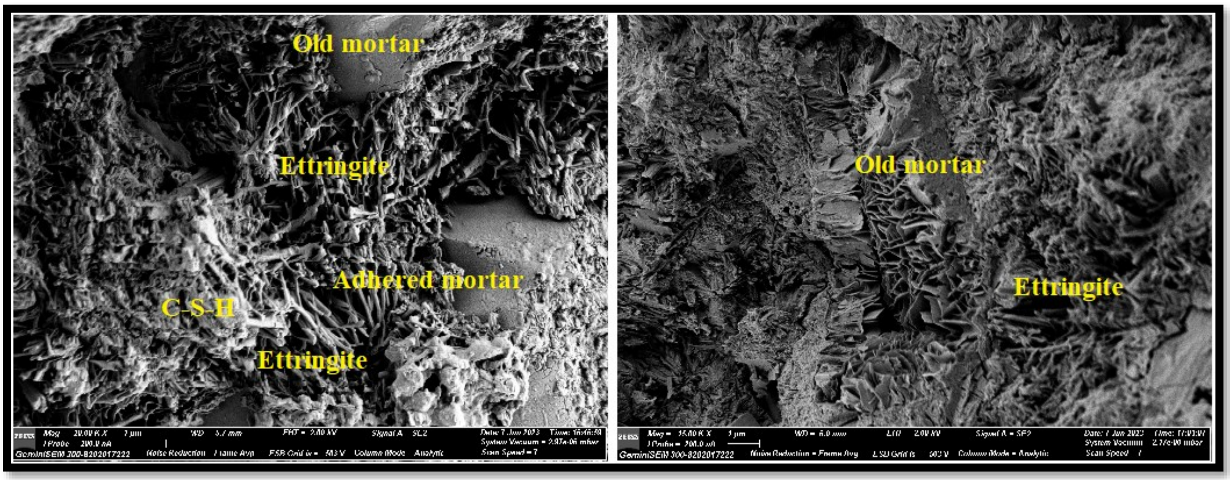

Fig. 13. SEM images of URAC samples

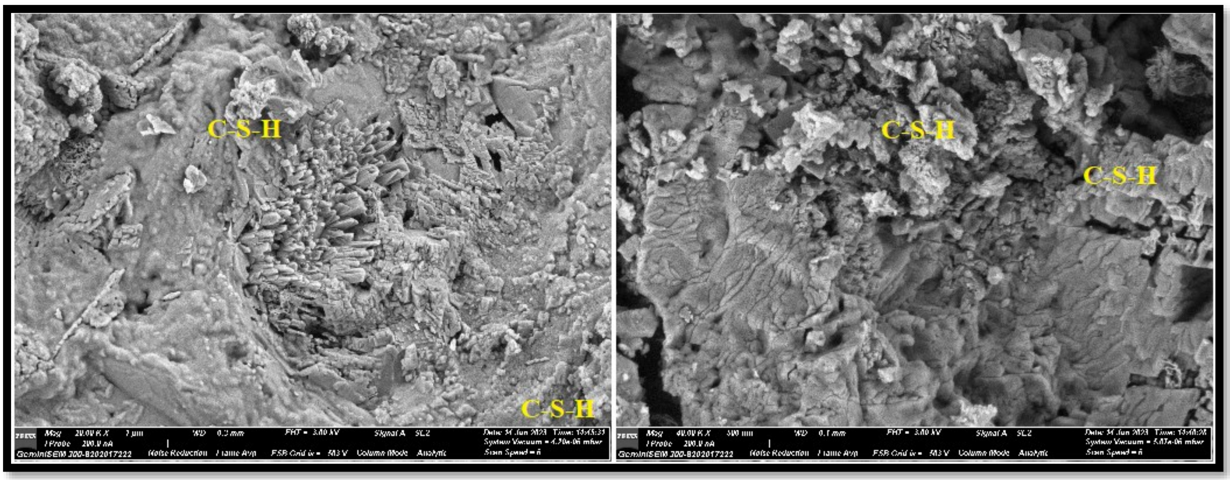

Fig. 14. SEM images of TR3 sample

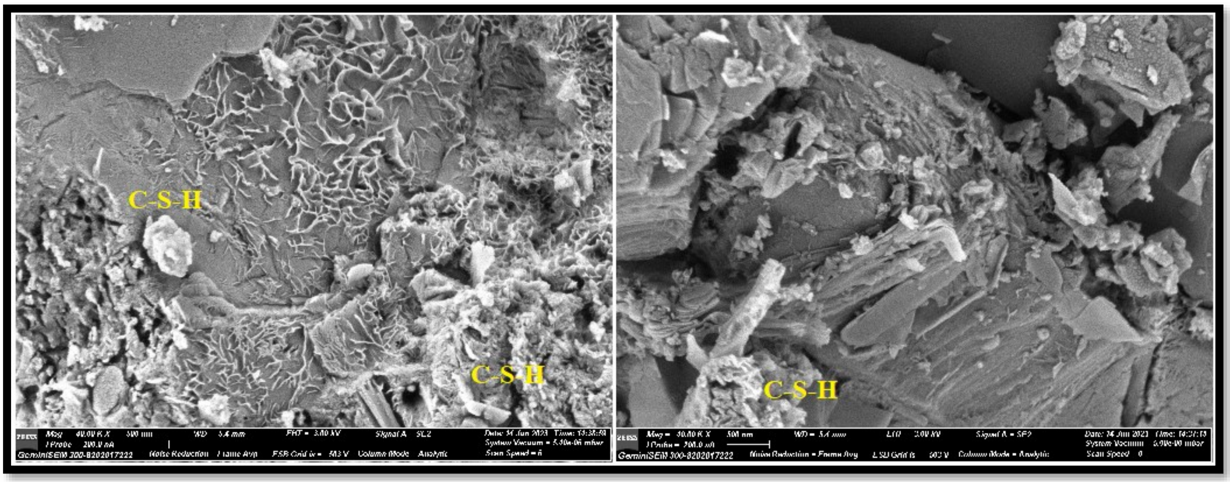

Fig. 15. SEM images of TR5 sample

3.2.6.2 Energy dispersive X-ray spectroscopy (EDAX)

The EDAX analysis of NAC, URAC, TR3 and TR5 are shown in the Figs. 16-19 respectively. For each of the concrete mix, area to point analysis is done to quantify the elemental composition. Fig. 20 illustrates a thorough elemental configuration and computed atomic weight ratios of calcium to silicate based on EDAX analysis data. It is well known that the Ca/Si ratio for dense concrete typically generally below 2. The Ca/Si atomic ratios of the TR3 and TR5 samples significantly decreased as compared to those of URAC, as can be seen. This might be attributable to the treatment approach, which encouraged the production of more C-S-H. This is a likely justification for using a multi-stage process that can change CH crystals into C-S-H, which later on strengthens RAC's strength and durability.

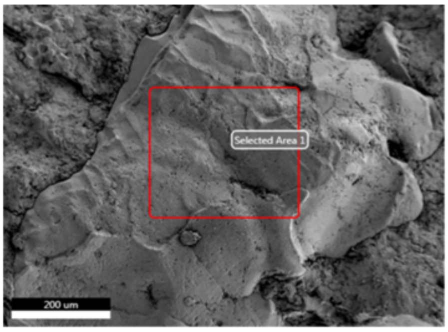

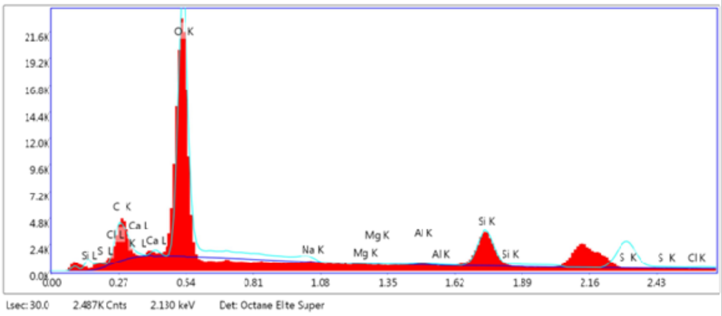

Element	Weight %	Atomic %	Net Int.	Error %
ClL	10.87	8.18	75.58	8.20
K L	28.04	19.14	283.76	6.39
C K	1.81	4.03	336.90	8.54
CaL	2.63	1.75	29.15	7.56
O K	21.63	36.10	4770.11	6.30
NaK	0.03	0.03	3.09	99.99
MgK	0.12	0.13	14.84	63.33
AlK	0.46	0.46	44.22	21.78
SiK	13.04	12.39	981.38	9.17
S K	21.37	17.79	643.16	13.41

Fig. 16 EDAX analysis of NAC

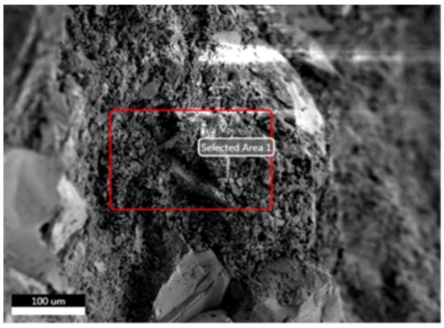

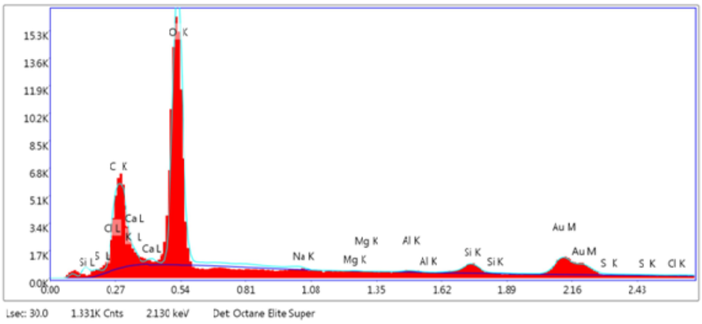

Element	Weight %	Atomic %	Net Int.	Error %
ClL	8.23	7.78	55.04	8.87
K L	33.28	28.53	288.50	6.77
C K	2.85	7.94	459.69	6.93
CaL	9.97	8.34	87.08	6.61
O K	18.86	39.52	3135.61	6.54
NaK	0.02	0.03	2.08	99.99
MgK	0.12	0.16	10.94	64.33
AlK	0.33	0.41	24.68	29.44
SiK	2.74	3.27	161.21	12.17
AuM	23.60	4.02	328.28	12.03
S K	0.00	0.00	0.03	99.99

Fig. 17 EDAX analysis of URAC

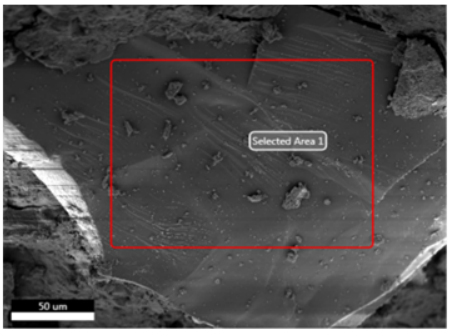

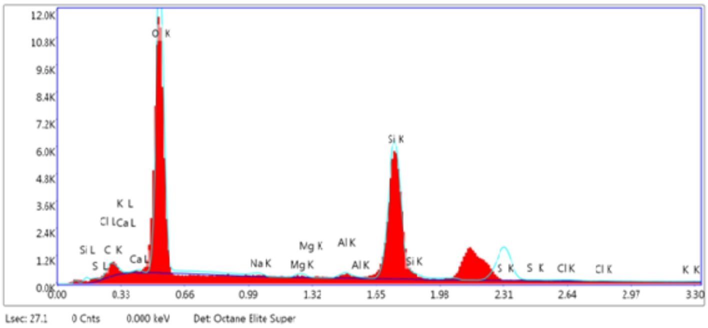

Element	Weight %	Atomic %	Net Int.	Error %
K L	14.21	9.06	60.69	7.48
C K	0.54	1.13	42.29	14.83
CaL	0.70	0.44	3.57	13.24
O K	24.22	37.76	2627.18	5.23
NaK	0.12	0.13	7.71	99.99
MgK	0.65	0.66	45.24	15.02
AlK	1.16	1.07	67.14	11.96
SiK	39.24	34.84	1875.95	6.00
S K	19.17	14.91	452.77	9.18
ClK	0.00	0.00	0.03	99.99

Fig. 18 EDAX analysis of TR3

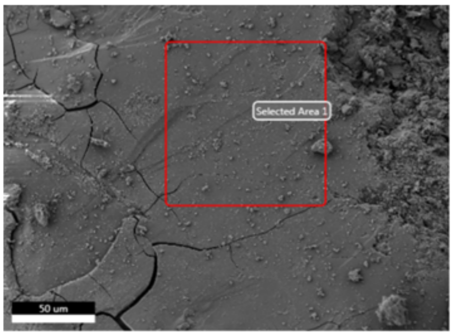

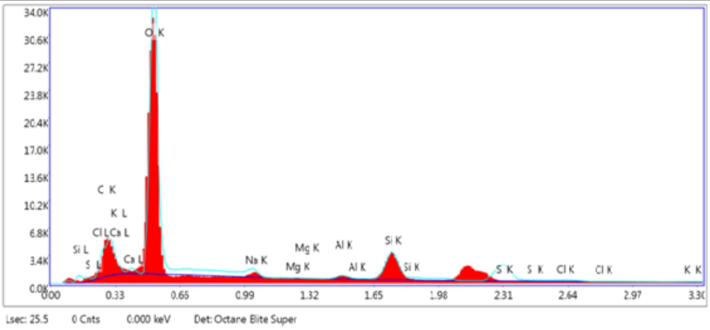

Element	Weight %	Atomic %	Net Int.	Error %
K L	38.69	25.76	540.67	5.30
C K	0.71	1.55	189.77	9.20
CaL	11.26	7.32	153.71	5.85
O K	29.42	47.87	8583.87	5.55
NaK	0.17	0.19	30.62	99.99
MgK	0.17	0.18	33.54	22.17
AlK	0.95	0.92	154.21	10.22
SiK	9.57	8.87	1303.77	6.78
S K	9.06	7.35	624.82	9.91
ClK	0.00	0.00	0.00	99.99

Fig. 19 EDAX analysis of TR5

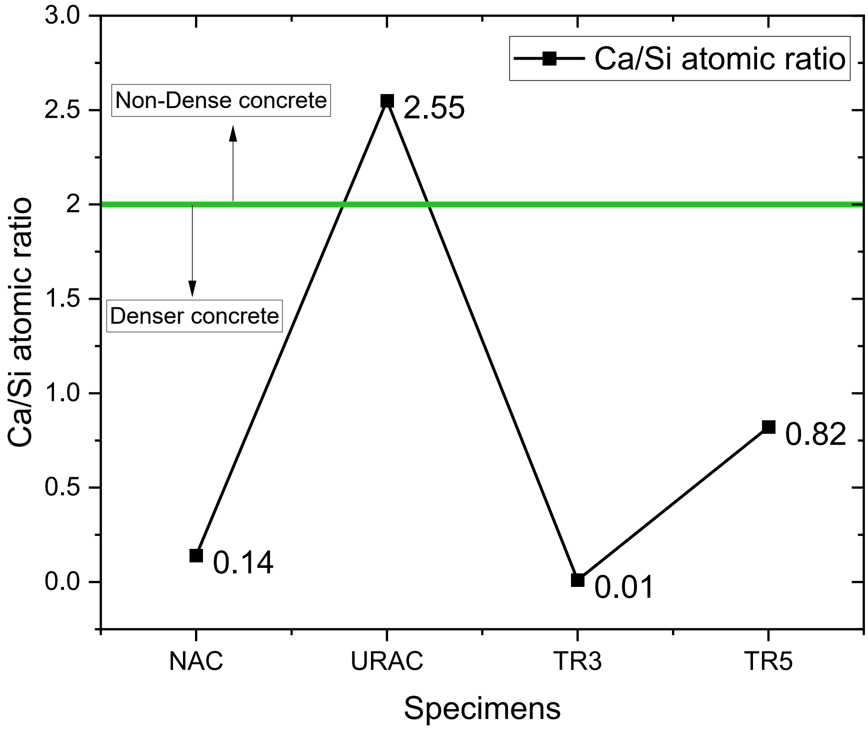

Fig. 20 Ca/Si atomic ratio of concrete specimens

3.2.6.3 Xray diffraction (XRD)

The XRD peaks of NAC, URAC, TR3 and TR5 mixes are illustrated in Fig. 21. The pattern of XRD for TR3 and TR5 showed the prominent peaks of calcium silicate hydrate in its hydrated phase (Calcium silicate hydroxide). A high intensity in the CSH peaks is observed for TR3 and TR5 with respect to untreated RAC. The prominent peaks in the untreated RAC are observed at an angle of 26.46, 20.69 (Quartz, SiO_2), 27.69 (Calcite, $CaCO_3$), 27.74° (unhydrated CSH). XRD peaks of TR3 and TR5 confirmed a slightly higher intensified peak of Calcium silicate hydroxide (27.78°) with respect to that of untreated RCA. However, TR3 and TR5 mixes showed relatively less intense portlandite peak (18.08°) with respect to URAC and NAC specimens. This is giving clear indication that TR3 and TR5 specimens contribute towards additional volumes of CSH fraction at microstructure levels. A detailed quantification of major XRD peaks is represented by Table 6.

Table 6. XRD peak analysis of treated and untreated RAC mixes

Peaks	NAC		URAC		TR3		TR5	
	2θ (Degree)	Intensity	2θ (Degree)	Intensity	2θ (Degree)	Intensity	2θ (Degree)	Intensity
1-Calcite ($CaCO_3$)	29.45, 39.51	1365, 1083	29.295	2069	29.29	1680	29.32, 46.97	1627, 1346
2-Quartz (SiO_2)	26.69, 20.95	4629, 1707	26.51, 20.76	8198, 2413	26.51, 20.71, 50.01	9943, 3246, 1887	26.51, 20.74, 50.04	9102, 2582, 1688
3- Calcium silicate hydroxide- ($Ca_4Si_5O_{13.5}(OH)_2$)	27.99	1744	27.381	2955	27.86	4006	27.78	3866
4-Potassium sulphate (K_2SO_4)	30.38	2170, 1710	30.33	1519	30.25	1921	30.33	1553
5- Portlandite ($Ca(OH)_2$)	34.13, 18.11	1115, 498	33.97, 17.93	2547, 3356	17.85	2015	34.00, 17,86	1997, 2123
6- Yeemlite ($Ca_4Al_6O_{12}SO_4$)	--	--	--	--	36.421	1927	--	--
7- Gypsum ($CaSO_4.2H_2O$)	--	--	--	--	--	--	--	--

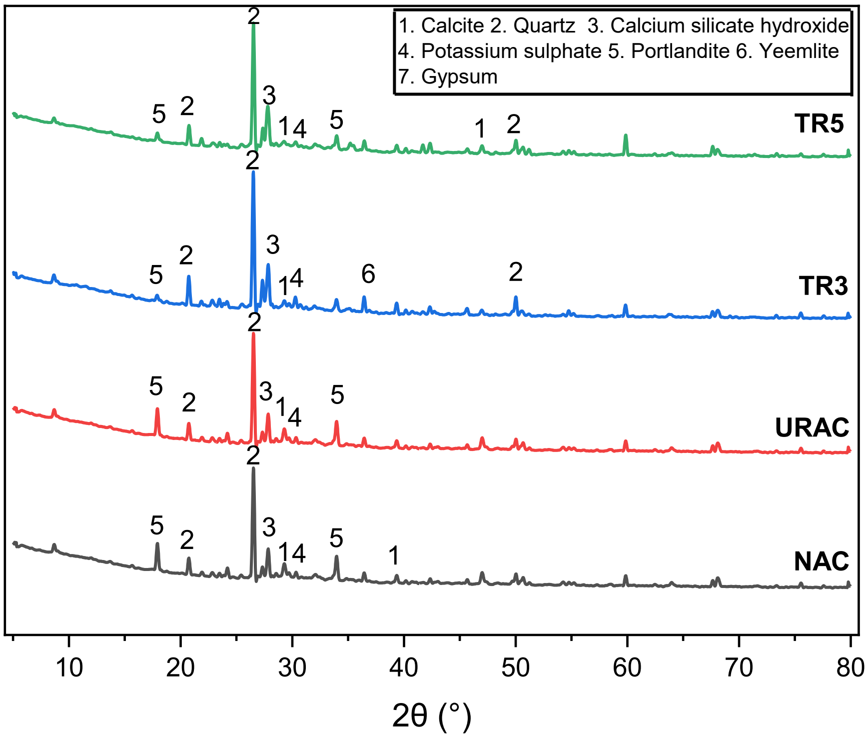

Fig. 21. XRD peaks of treated and untreated RAC mixes

1-Calcite ($CaCO_3$), 2-Quartz (SiO_2), 3- Calcium silicate hydroxide- ($Ca_4Si5O_{13.5}(OH)_2$), 4-Potassium sulphate (K_2SO_4), 5- Portlandite ($Ca(OH)_2$),6- Yeemlite ($Ca_4Al_6O_{12}SO_4$), 7-Gypsum ($CaSO_4.2H_2O$)

3.2.6.4 Fourier-transform infrared spectroscopy (FTIR)

Fig. 22 shows the FTIR spectra of the NAC, URAC, TR3, and TR5 mixtures. In RAC samples, there was no significant peak at wavelength 3640 cm^{-1} that conformed to the O-H stretching bond of portlandite. This finding is consistent with the research done by [46]. This was attributed to the calcium carbonate phases that resulted from portlandite's interaction with ambient carbon dioxide. The increasing amount of water molecules in the samples is what caused the stretching vibration of O-H between 1600 and 1690 cm^{-1} [46,47]. The asymmetric stretching vibration of the C-O bond, the symmetric stretching vibration of the Si-O bond, the symmetric stretching vibration of the Si-O bond, and the unhydrated cement, respectively, have peak intervals between 1400 and 1440 cm^{-1}, 1000 and 950 cm^{-1}, 780 and 770 cm^{-1}, and 595 and 570 cm^{-1}. Table 7 provides more information on peak locations and their functional groupings.

The distinctive peaks at 972 cm^{-1}, 966 cm^{-1}, 784 cm^{-1}, and 773 cm^{-1} are gradually lost as the amount of substituted RCA is increased, indicating that the interaction between the modified RCA and cementitious composites consumed the calcite and CH. According to the findings of the FTIR research, RA treated with sodium silicate can react with the calcite and CH in the cementitious matrix to form a calcium-sodium silicate complex.

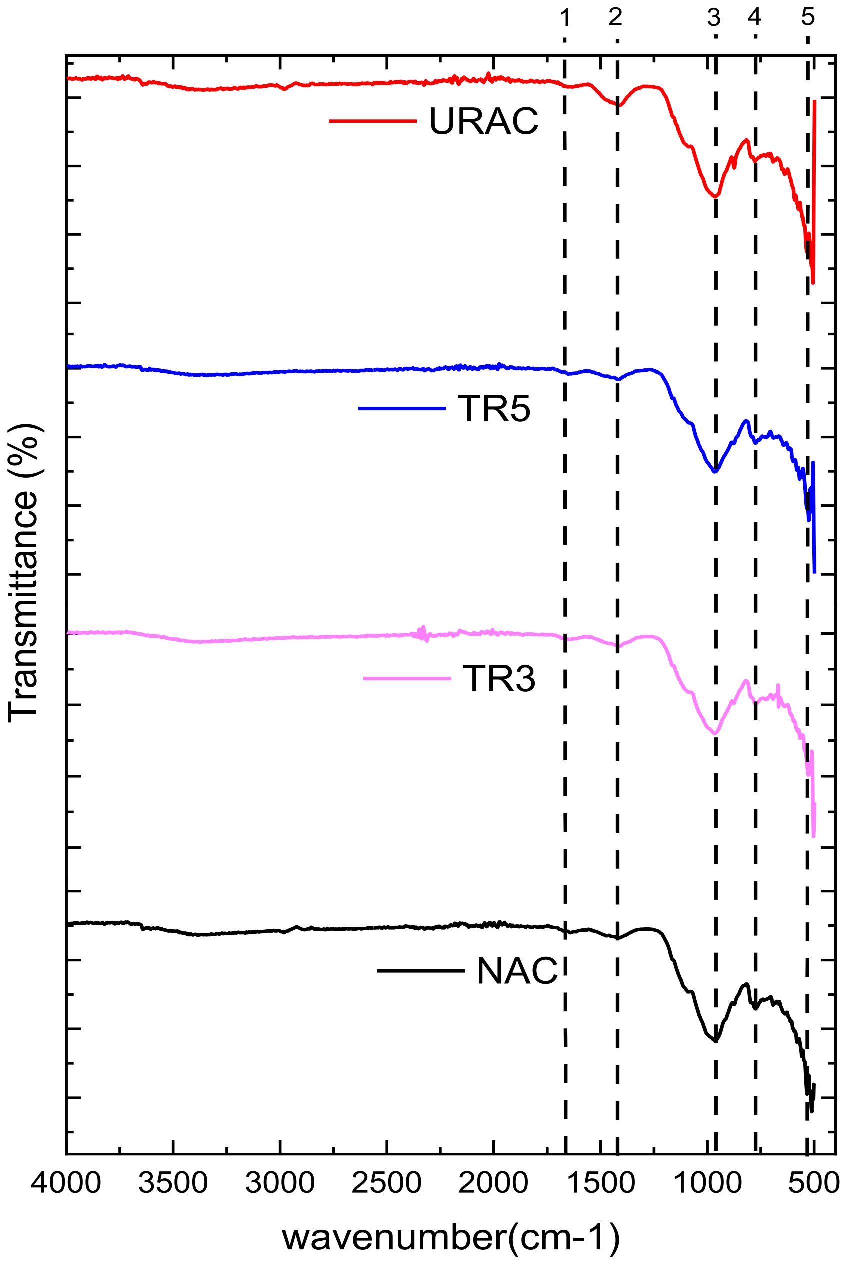

Fig. 22. FT-IR spectrum of treated and untreated RAC mixes

Table 7 Progression of Peaks for natural and treated RAC (wave number:cm^{-1})

Wave Numbers	Functional group	NAC	TR3	TR5	URAC	References
1	O-H	1660	1670	1681	1668	[42]
2	C-O	1426	1422	1434	1404	[43]
3	Si-O Asymmetric stretching	970	972	966	960	[43–45]
4	Si-O Symmetric stretching	777	784	773	776	[43–45]
5	Unhydrated* cement	--	--	--	--	[43]

(* Unclear Peak intensity)

3.2.6.5 Thermogravimetry analysis (TGA)

The derivative of thermogravimetry (DTG) curve shows the temperature borders for the decomposition of particular compounds, whereas Fig. 23 depicts the TG curve that illustrates the existence of thermogravimetric mass loss for treated RA specimens throughout the heating progression between 25°C-900°C.

Fig. 23 shows that there are a number of endothermic peaks between the temperature ranges of 25°C and 900°C. The temperature ranges of 25–50 ºC, 50–120 ºC, and 120–150 ºC, which are connected to the loss of free water molecules, ettringites, and gypsum, respectively, can be further split from the principal endothermic peak till 200 ºC. The calcium hydroxide (CH) is dehydroxylated at a temperature range of 400–500 ºC, where a second significant endothermic peak was seen. The decarbonation of calcium carbonates (around 600–800 ºC) causes the third significant peak [2].

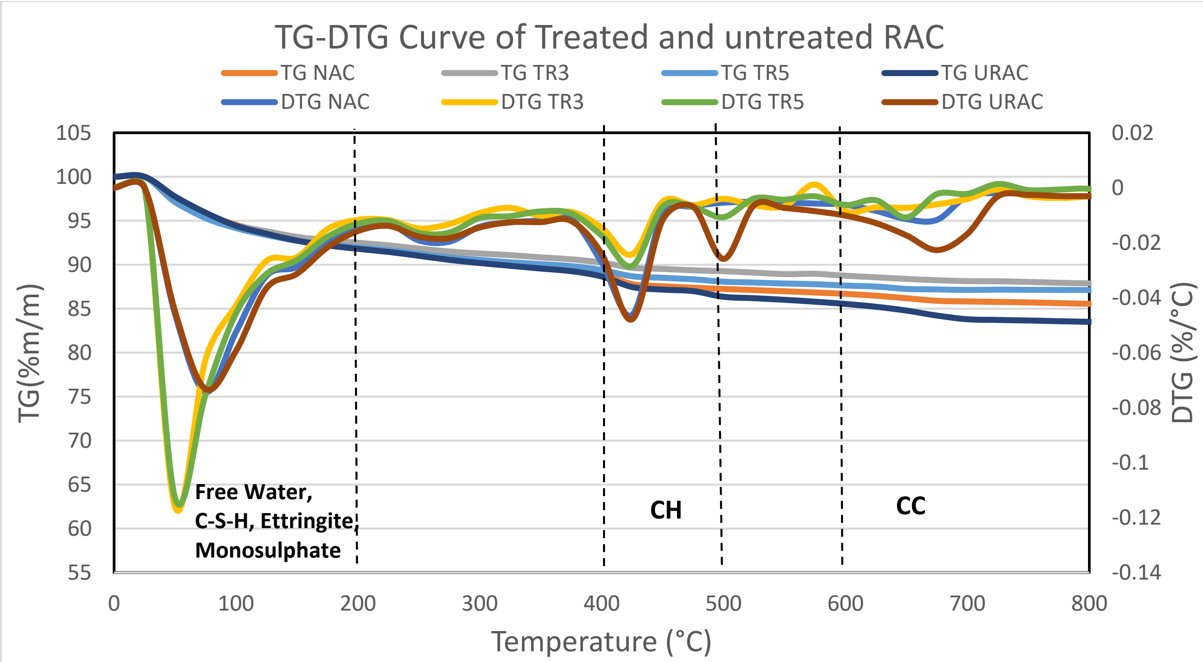

Fig. 23. TG-DTG curves of treated and untreated RAC mixes

It should be mentioned that in this investigation, the following equations—equations 2, 3, and 4 at particular temperature bounds are taken into account to regulate the mass loss from TG-DTG. Quantified data is shown in Table 8. The symbols used in the following equation stand for the proportion of calcium hydroxide that has been decomposed (CH%), while Wn% and CC%, respectively, reflect the percentages of bound water and calcium carbonate that have produced.

$$CH\% = (\%W_{CH}) \times (\frac{M_{CH}}{M_{H_2O}}) = (\%W_{CH} \times \frac{74}{18}) \quad (2)$$

$$W_n\% = W_T - W_{CH} \quad (3)$$

$$CC\% = (\%W_{CC}) \times (\frac{M_{CC}}{M_{CO2}}) = (\%W_{CC} \times \frac{100}{44}) \quad (4)$$

Table 8 TGA analysis of distinct phases in hydration products

Mixes	Temperature Boundary							Quantified amount of phase composition		
	50 °C	400 °C	430 °C	460 °C	500 °C	600 °C	700 °C	Wn %	CH%	CC%
URAC	97.75	88.66	--	--	86.34	85.53	83.79	11.64	9.53	3.94
TR3	97.90	89.39	--	--	89.26	88.74	88.13	9.64	0.53	1.38
TR5	97.75	89.39	--	--	88.06	87.62	87.13	9.29	5.90	1.11
NAC	97.20	89.24	--	--	87.36	86.86	85.81	9.51	7.76	2.38

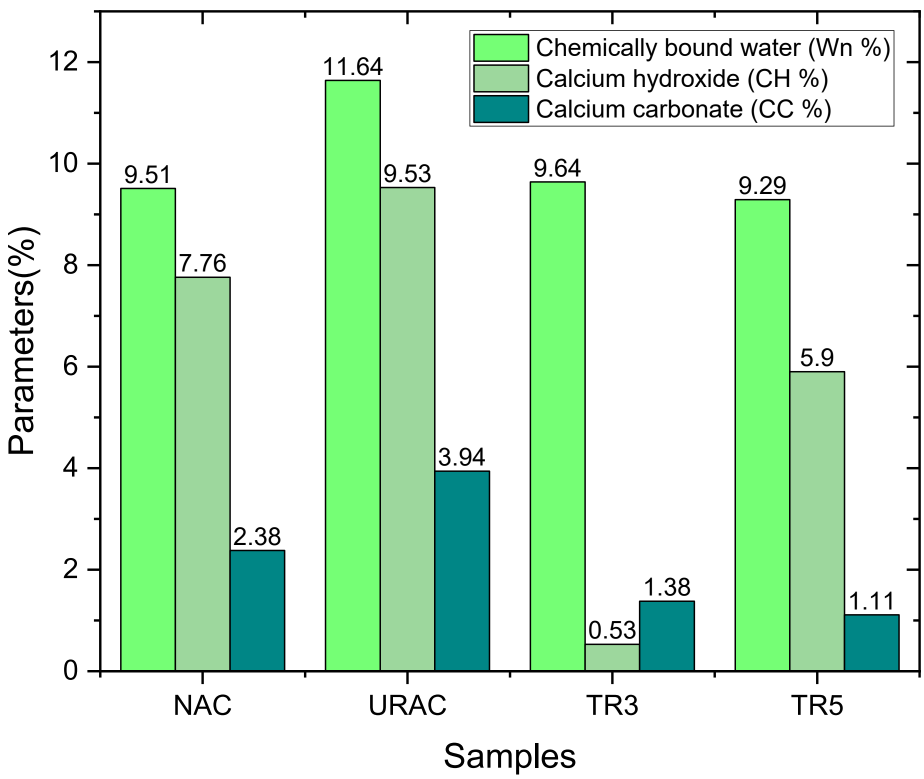

Fig. 24. Quantified percentages of W_n, CH and CC from TGA results of treated and untreated RAC mixes

Fig. 24 exemplifies the quantified proportion of hydration products such as calcium hydroxide (CH%), calcium carbonate (CC%) and bound water (W_n %). It is to be noted that the lower values of CH phase for the treated RAC mixes i.e., TR3 and TR5 (lowest for TR3) specimens indicates the development of stable C-S-H phases as a consequence of induced chemical response amid sodium silicate treated RCA with CH crystals (Equation 1). TR3 showed lowest values of CH crystals among two substituted mixes indicates that 35% substitution of treated RCA is optimum among the two mixes, contributing to higher volumes of C-S-H fraction at microstructure levels. This may be accredited to the minimization in the adhered mortar fractions in RCA due to mechanical scrubbing.

4. Cost Estimation and Technoeconomic analysis

The elemental costs of all the materials were gathered from national and global markets in order to determine the cost of developing one cubic metre of each of the concrete combinations (URAC, TR3 and TR5) taken into consideration in the current work.

The expense induced in multi stage jaw crushing, los Angeles test machine and concrete mixing were taken into consideration by calculating the cost of the energy used by the respective machinery. The price of RAC per cubic meter is shown in Table 9. In addition, the cost involved for producing per unit compressive strength of concrete is also evaluated for carrying out techno-economic analysis of the produced concrete specimens.

As shown by the data in Table 9, the cost/strength of TR3 mix decreased by 0.2 %, whereas for TR5 mix, the cost/strength increased by 10%. In addition, the TR3 mix is found to outperform TR5 mix in terms of mechanical, microstructure and durability properties. Even though it is estimated that TR5 mixes are slightly expansive, the microstructure studies revealed to illustrate a dense concrete alongside satisfactory durability performance. The longer useful service life of the structures will increase their durability, which will reduce total cost. The mechano-chemical method of treating the RA would be highly appropriate to generate RAC for usage in chloride prone areas and subsequently it can provide resistance to water absorption at the same time.

Table 9 Cost estimation for different RAC mixes

Particulars	Unit Cost (₹/ton)	URAC	TR3	TR5
Cement	3700	1897.1	1897.1	1897.1
Fine aggregates	400	273	273	273
NA	350	--	232	174.8
URA (Processing stage)	155	155	--	--
MS+SS_RA	1230.5	--	370	616
Water	85.1	17	17	17
Mix energy consumption (₹/kWh)	22.8	50.6	50.6	50.6
Total cost (₹/m^3)		2392.7	2839.7	3028.5
Cost (₹)/MPa		56.67	56.55	62.34
Changes in Cost / MPa		--	0.2% fall	10% rise

NA- Natural aggregate, URA- Untreated RA, MS+SS_RA- Mechano-chemical treated RA

Conclusion

The existing research work examines the feasibility of mechanical-chemical treatment for the processed RCA as a partial substitution for natural coarse aggregate in concrete works. Demolished concrete was processed under multi crushing cycles through jaw crusher that was followed by two stage treatment through mechanical-chemical methods. The two-stage treatment initiated through los angeles abrasion followed by sodium silicate immersion of processed aggregates. The usefulness of mechanical-chemical treatment method was assessed in terms of physical properties of aggregates, mechanical and durability characteristics of treated and untreated RAC mixes. In addition, the microstructural analysis is carried out through SEM, EDAX, XRD, FTIR and TG-DTA. Based on the outcomes of this research work, the subsequent inferences can be drawn

1. Multi stage processing and mechano-chemical treatment enhances the quality and physical performance of RCA.
2. The desired workability is achieved at 35% replacement of two-stage treated RA. A similar trend is observed where the RAC mixes at identical substitution percentage illustrated highest compressive strength at the age of 7 days and 28 days.
3. The splitting tensile strength decreases with additional replacement of RCA. However, a comparable strength to control concrete is achieved when the treated RA substituted the raw RA at 35% replacement levels.
4. With respect to the flexural strength development, 100% replacement of untreated RA shows the lowest value which is nearly equal to half of the value of control concrete. The flexural strength is almost equal in cases of 35% and 50% replacement.
5. TR3 and TR5 specimen illustrated highest resistivity to chloride penetration as compared to other mixes whereas URAC mix is found to be prone to chloride attack due to presence of additional porous sites whereas in water sorptivity tests, the treated RAC mixes are found to demonstrate least absorption at both the stages.
6. From a microstructural perspective, the mechano-chemical treatment approach helped generate more calcium silicate hydrate (C-S-H). This is the most likely justification for using a multi-stage process that can change CH crystals into C-S-H, which later enhances the strength and durability of RAC mixtures.
7. After analyzing all the result, it can be concluded that 35% is the optimum replacement level of multi stage processed recycled concrete aggregates (RCA) in RAC mixes with adoption of two stage treatment approach.

Future Scope and Challenges

Concrete comprising treated RA performed better because mechano-chemical treatment has been found to change the fundamental properties of aggregates (specific gravity and water absorption, in particular). Untreated RA has a lower bulk density and a higher water absorption rate, which impacts both the fresh and hardened concrete's characteristics. The durability of RAC, which contributes to greater chloride intrusion and water sorptivity, is a crucial property that is substantially impacted by the porous nature of RA. Quality improvements in RA can be accomplished by two stages of treatment that further enhance the mechanical and durability characteristics of RAC. The positive findings of this work motivate further investigation of the microstructure of RAC, including varying concentrations of treated RA. Future concrete elements with a higher surface area-to-depth ratio, like rigid pavements, and in low to high-load-bearing concrete elements might benefit especially from studying such parameters. The mix design approach from the standpoint of residual mortar fractions on RA, which in turn depends on the choice of adopted treatment methods, is a further topic of research that has to be investigated. Such a study would be helpful in producing an optimum mix for the desired qualities of concrete. Removing any remanent mortar will improve the structure and surface characteristics, which will result in a decrease in absorption capacity and an increase in specific gravity. These essential qualities are crucial for mix design and, as a result, affect the properties of the resulting concrete, as this research has shown. Pretreatment's potential to remove adherent mortar promotes the use of these materials in a variety of structural and non-structural concrete components, lessening the demand on natural aggregate resources. Concrete-related CO_2 emissions must be decreased on a qualitative level. The intangible benefits (in terms of sustainability) acquired from utilizing RA instead of natural aggregates (in concrete) are sufficient enough to warrant consideration, even though the economic benefits are worthwhile investigating. Scalability comes next after the usefulness of pretreatment has been established. Pretreatment should be implemented at the aggregate recycling plants, and other ways and means should be explored. For future waste management system enhancement, the degree of reusability of pretreatment solutions (after usage) also needs to be studied. The mortar remnants that have been filtered and then allowed to dry can be utilised as fine aggregate fillers in concrete or base/sub-base layers for road pavements.

References

[1] M.V.A. Florea, H.J.H. Brouwers, Properties of various size fractions of crushed concrete related to process conditions and re-use, Cem Concr Res. 52 (2013) 11–21. https://doi.org/10.1016/j.cemconres.2013.05.005.

[2] S. S. Trivedi, K. Snehal, B.B. Das, S. Barbhuiya, A comprehensive review towards sustainable approaches on the processing and treatment of construction and demolition waste, Constr Build Mater. 393 (2023) 132125. https://doi.org/10.1016/j.conbuildmat.2023.132125.

[3] C. Liang, B. Pan, Z. Ma, Z. He, Z. Duan, Utilization of CO_2 curing to enhance the properties of recycled aggregate and prepared concrete: A review, Cem Concr Compos. 105 (2020). https://doi.org/10.1016/j.cemconcomp.2019.103446.

[4] B. Zhan, C.S. Poon, Q. Liu, S. Kou, C. Shi, Experimental study on CO_2 curing for enhancement of recycled aggregate properties, Constr Build Mater. 67 (2014) 3–7. https://doi.org/10.1016/j.conbuildmat.2013.09.008.

[5] X.-F. Chen, C.-J. Jiao, Microstructure and physical properties of concrete containing recycled aggregates pre-treated by a nano-silica soaking method, Journal of Building Engineering. 51 (2022). https://doi.org/10.1016/j.jobe.2022.104363.

[6] R. Purushothaman, R.R. Amirthavalli, L. Karan, Influence of Treatment Methods on the Strength and Performance Characteristics of Recycled Aggregate Concrete, Journal of Materials in Civil Engineering. 27 (2015) 04014168. https://doi.org/10.1061/(asce)mt.1943-5533.0001128.

[7] P. Saravanakumar, K. Abhiram, B. Manoj, Properties of treated recycled aggregates and its influence on concrete strength characteristics, Constr Build Mater. 111 (2016) 611–617. https://doi.org/10.1016/j.conbuildmat.2016.02.064.

[8] A. Mistri, S.K. Bhattacharyya, N. Dhami, A. Mukherjee, S. V. Barai, A review on different treatment methods for enhancing the properties of recycled aggregates for sustainable construction materials, Constr Build Mater. 233 (2020). https://doi.org/10.1016/j.conbuildmat.2019.117894.

[9] E. Güneyisi, M. Gesoğlu, Z. Algın, H. Yazıcı, Effect of surface treatment methods on the properties of self-compacting concrete with recycled aggregates, Constr Build Mater. 64 (2014). https://doi.org/10.1016/j.conbuildmat.2014.04.090.

[10] P. Zhan, J. Xu, J. Wang, J. Zuo, Z. He, A review of recycled aggregate concrete modified by nanosilica and graphene oxide: Materials, performances and mechanism, J Clean Prod. 375 (2022). https://doi.org/10.1016/j.jclepro.2022.134116.

[11] L. Wang, J. Wang, X. Qian, P. Chen, Y. Xu, J. Guo, An environmentally friendly method to improve the quality of recycled concrete aggregates, Constr Build Mater. 144 (2017). https://doi.org/10.1016/j.conbuildmat.2017.03.191.

[12] N.K. Bui, T. Satomi, H. Takahashi, Mechanical properties of concrete containing 100% treated coarse recycled concrete aggregate, Constr Build Mater. 163 (2018). https://doi.org/10.1016/j.conbuildmat.2017.12.131.

[13] M.A.T. Alsheyab, Recycling of construction and demolition waste and its impact on climate change and sustainable development, International Journal of Environmental Science and Technology. 19 (2022) 2129–2138. https://doi.org/10.1007/s13762-021-03217-1.

[14] A.A. Bahraq, J. Jose, M. Shameem, M. Maslehuddin, A review on treatment techniques to improve the durability of recycled aggregate concrete: Enhancement mechanisms, performance and cost analysis, Journal of Building Engineering. 55 (2022). https://doi.org/10.1016/j.jobe.2022.104713.

[15] R.Md. Faysal, M. Maslehuddin, M. Shameem, S. Ahmad, S.K. Adekunle, Effect of mineral additives and two-stage mixing on the performance of recycled aggregate concrete, J Mater Cycles Waste Manag. 22 (2020) 1587–1601. https://doi.org/10.1007/s10163-020-01048-9.

[16] P. Rattanachu, P. Toolkasikorn, W. Tangchirapat, P. Chindaprasirt, C. Jaturapitakkul, Performance of recycled aggregate concrete with rice husk ash as cement binder, Cem Concr Compos. 108 (2020) 103533. https://doi.org/10.1016/j.cemconcomp.2020.103533.

[17] M. Koushkbaghi, M.J. Kazemi, H. Mosavi, E. Mohseni, Acid resistance and durability properties of steel fiber-reinforced concrete incorporating rice husk ash and recycled aggregate, Constr Build Mater. 202 (2019) 266–275. https://doi.org/10.1016/j.conbuildmat.2018.12.224.

[18] H. Sasanipour, F. Aslani, J. Taherinezhad, Effect of silica fume on durability of self-compacting concrete made with waste recycled concrete aggregates, Constr Build Mater. 227 (2019) 116598. https://doi.org/10.1016/j.conbuildmat.2019.07.324.

[19] W. Hu, S. Li, C. Song, Z. Chen, L. Chen, Y. Yang, W. Luo, A Laboratory Analysis of Chloride Ions Penetration in Recycled Aggregates Concrete Admixed with Ground Granulated Blast Furnace Slag, IOP Conf Ser Mater Sci Eng. 611 (2019) 012051. https://doi.org/10.1088/1757-899X/611/1/012051.

[20] K. Kim, M. Shin, S. Cha, Combined effects of recycled aggregate and fly ash towards concrete sustainability, Constr Build Mater. 48 (2013) 499–507. https://doi.org/10.1016/j.conbuildmat.2013.07.014.

[21] Y. Zheng, Y. Zhang, P. Zhang, Methods for improving the durability of recycled aggregate concrete: A review, Journal of Materials Research and Technology. 15 (2021) 6367–6386. https://doi.org/10.1016/j.jmrt.2021.11.085.

[22] W.M. Shaban, K. Elbaz, J. Yang, B.S. Thomas, X. Shen, L. Li, Y. Du, J. Xie, L. Li, Effect of pozzolan slurries on recycled aggregate concrete: Mechanical and durability performance, Constr Build Mater. 276 (2021) 121940. https://doi.org/10.1016/j.conbuildmat.2020.121940.

[23] S.-C. Kou, B. Zhan, C.-S. Poon, Use of a CO2 curing step to improve the properties of concrete prepared with recycled aggregates, Cem Concr Compos. 45 (2014) 22–28. https://doi.org/10.1016/j.cemconcomp.2013.09.008.

[24] A. Akbarnezhad, K.C.G. Ong, M.H. Zhang, C.T. Tam, T.W.J. Foo, Microwave-assisted beneficiation of recycled concrete aggregates, Constr Build Mater. 25 (2011) 3469–3479. https://doi.org/10.1016/j.conbuildmat.2011.03.038.

[25] L. Wang, J. Wang, X. Qian, P. Chen, Y. Xu, J. Guo, An environmentally friendly method to improve the quality of recycled concrete aggregates, Constr Build Mater. 144 (2017) 432–441. https://doi.org/10.1016/j.conbuildmat.2017.03.191.

[26] L. Li, D. Xuan, A.O. Sojobi, S. Liu, C.S. Poon, Efficiencies of carbonation and nano silica treatment methods in enhancing the performance of recycled aggregate concrete, Constr Build Mater. 308 (2021) 125080. https://doi.org/10.1016/j.conbuildmat.2021.125080.

[27] S. Ahmad, M. Maslehuddin, M. Shameem, R.Md. Faysal, S.K. Adekunle, Effect of abrasion and chemical treatment of recycled aggregate on the workability, strength, and durability properties of concrete, European Journal of Environmental and Civil Engineering. 26 (2022) 3276–3291. https://doi.org/10.1080/19648189.2020.1797886.

[28] G. Dimitriou, P. Savva, M.F. Petrou, Enhancing mechanical and durability properties of recycled aggregate concrete, Constr Build Mater. 158 (2018). https://doi.org/10.1016/j.conbuildmat.2017.09.137.

[29] H. Zhang, Y. Zhao, T. Meng, S.P. Shah, Surface Treatment on Recycled Coarse Aggregates with Nanomaterials, Journal of Materials in Civil Engineering. 28 (2016). https://doi.org/10.1061/(ASCE)MT.1943-5533.0001368.

[30] B.J. Zhan, D.X. Xuan, W. Zeng, C.S. Poon, Carbonation treatment of recycled concrete aggregate: Effect on transport properties and steel corrosion of recycled aggregate concrete, Cem Concr Compos. 104 (2019) 103360. https://doi.org/10.1016/j.cemconcomp.2019.103360.

[31] F. Shaikh, V. Chavda, N. Minhaj, H.S. Arel, Effect of mixing methods of nano silica on properties of recycled aggregate concrete, Structural Concrete. 19 (2018) 387–399. https://doi.org/10.1002/suco.201700091.

[32] S. Gupta, H. Agrawal, S. Chaudhary, Thermo-mechanical treatment as an upcycling strategy for mixed recycled aggregate, Constr Build Mater. 398 (2023) 132471. https://doi.org/10.1016/j.conbuildmat.2023.132471.

[33] IS 516, Method of Tests for Strength of Concrete, Bureau of Indian Standards, New Delhi, 1959.

[34] IS 1199, Methods of sampling and analysis of concrete, Bureau of Indian Standards, New Delhi, 1959.

[35] IS 5816, Method of Test Splitting Tensile Strength of Concrete, Bureau of Indian Standards, New Delhi, 1999.

[36] Standard Test Method for Electrical Indication of Concrete's Ability to Resist Chloride Ion Penetration, (2012). https://doi.org/10.1520/C1202-12.

[37] Standard Test Method for Measurement of Rate of Absorption of Water by Hydraulic-Cement Concretes Specification for Reference Masses and Devices for Determining

Mass and Volume for Use in the Physical Testing of Hydraulic Cements, (2004). www.astm.org.

[38] E. Güneyisi, M. Gesoğlu, Z. Algın, H. Yazıcı, Effect of surface treatment methods on the properties of self-compacting concrete with recycled aggregates, Constr Build Mater. 64 (2014). https://doi.org/10.1016/j.conbuildmat.2014.04.090.

[39] IS 383, Coarse and Fine Aggregate for Concrete - Specification, Bureau of Indian Standards, New Delhi, 2016.

[40] Z. He, A. Shen, W. Wang, X. Zuo, J. Wu, Evaluation and optimization of various treatment methods for enhancing the properties of brick-concrete recycled coarse aggregate, J Adhes Sci Technol. 36 (2022) 1060–1080. https://doi.org/10.1080/01694243.2021.1956210.

[41] K. Pandurangan, A. Dayanithy, S. Om Prakash, Influence of treatment methods on the bond strength of recycled aggregate concrete, Constr Build Mater. 120 (2016) 212–221. https://doi.org/10.1016/j.conbuildmat.2016.05.093.

[42] S. Shahbazpanahi, M.K. Tajara, R.H. Faraj, A. Mosavi, Studying the C–H crystals and mechanical properties of sustainable concrete containing recycled coarse aggregate with used nano-silica, Crystals (Basel). 11 (2021). https://doi.org/10.3390/cryst11020122.

[43] S. Pradhan, S. Kumar, S. V. Barai, Understanding the behavior of recycled aggregate concrete by using thermogravimetric analysis, Frontiers of Structural and Civil Engineering. 14 (2020) 1561–1572. https://doi.org/10.1007/s11709-020-0640-5.

[44] M. Horgnies, J.J. Chen, C. Bouillon, Overview about the use of fourier transform infrared spectroscopy to study cementitious materials, in: WIT Transactions on Engineering Sciences, WITPress, 2013: pp. 251–262. https://doi.org/10.2495/MC130221.

[45] F. Puertas, S. Goñi, M.S. Hernández, C. Varga, A. Guerrero, Comparative study of accelerated decalcification process among C 3S, grey and white cement pastes, Cem Concr Compos. 34 (2012) 384–391. https://doi.org/10.1016/j.cemconcomp.2011.11.002.